



**Tran-SET**

**Transportation Consortium of South-Central States**

*Solving Emerging Transportation Resiliency, Sustainability, and Economic Challenges through the Use of Innovative Materials and Construction Methods: From Research to Implementation*

# **Integrated Full-Scale Physical Experiments and Numerical Modeling of the Performance and Rehabilitation of Highway Embankments**

**Project No. 18GTLU06**

**Lead University: Louisiana State University**

**Collaborative Universities: University of Texas at Arlington**

**Final Report  
September 2019**

### **Disclaimer**

The contents of this report reflect the views of the authors, who are responsible for the facts and the accuracy of the information presented herein. This document is disseminated in the interest of information exchange. The report is funded, partially or entirely, by a grant from the U.S. Department of Transportation's University Transportation Centers Program. However, the U.S. Government assumes no liability for the contents or use thereof.

### **Acknowledgements**

The discussions and feedback by the Louisiana Department of Transportation and Development and Texas Department of Transportation are greatly appreciated.

## TECHNICAL DOCUMENTATION PAGE

<b>1. Project No.</b> 18GTLSU06	<b>2. Government Accession No.</b>	<b>3. Recipient's Catalog No.</b>	
<b>4. Title and Subtitle</b>  Integrated Full-Scale Physical Experiments and Numerical Modeling of the Performance and Rehabilitation of Highway Embankments	<b>5. Report Date</b> Sept. 2019		
	<b>6. Performing Organization Code</b>		
<b>7. Author(s)</b> PI: Navid H. Jafari <a href="https://orcid.org/0000-0002-4394-3776">https://orcid.org/0000-0002-4394-3776</a> Co-PI: Anand J. Puppala <a href="https://orcid.org/0000-0003-0435-6285">https://orcid.org/0000-0003-0435-6285</a> Post-doc: Sayantan Chakraborty <a href="https://orcid.org/0000-0002-6809-5953">https://orcid.org/0000-0002-6809-5953</a> GRA: Burak Boluk <a href="https://orcid.org/0000-0002-1730-6212">https://orcid.org/0000-0002-1730-6212</a>	<b>8. Performing Organization Report No.</b>		
<b>9. Performing Organization Name and Address</b> Transportation Consortium of South-Central States (Tran-SET) University Transportation Center for Region 6 3319 Patrick F. Taylor Hall, Louisiana State University, Baton Rouge, LA 70803	<b>10. Work Unit No. (TRAIS)</b>		
	<b>11. Contract or Grant No.</b> 69A3551747106		
<b>12. Sponsoring Agency Name and Address</b> United States of America Department of Transportation Research and Innovative Technology Administration	<b>13. Type of Report and Period Covered</b> Final Research Report Mar. 2018 – Mar. 2019		
	<b>14. Sponsoring Agency Code</b>		
<b>15. Supplementary Notes</b> Report uploaded and accessible at <a href="http://transet.lsu.edu/">Tran-SET's website (http://transet.lsu.edu/)</a> .			
<b>16. Abstract</b> <p>The study aimed to fundamentally understand how soil strength and hydraulic properties are impacted by recurring cycles of wetting and drying induced by climate variability, with the practical implication of forecasting the stability of highway embankment slopes. The review of literature on the effects of long-term cyclic wetting-drying phases on hydro-mechanical properties of clayey soils suggests that only a few cycles of wetting and drying can impact the strength and hydraulic conductivity, where the latter can increase several orders of magnitude. Laboratory model-scale experiments of Louisiana and Texas soils are still ongoing and will relate the laboratory test results to weathering cycles by accounting for parameters such as rainfall intensity and duration, evapotranspiration, temperature, and relative humidity. The objective of the laboratory testing was to determine the strength and unsaturated soil properties of samples collected from laboratory model-scale experiments and to investigate the subsequent changes in the hydro-mechanical properties of those clayey soils. For example, shrinkage test results provided a measure of the propensity and extent of strength loss incurred by a soil specimen when exposed to weathering cycles. Numerical modeling of highway embankments with material properties and test results obtained from lab testing were used to predict the factor of safety for an embankment in Texas.</p>			
<b>17. Key Words</b> Shallow slope failure, Weathering, Softening, Soil water retention curve	<b>18. Distribution Statement</b> No restrictions. This document is available through the National Technical Information Service, Springfield, VA 22161.		
<b>19. Security Classif. (of this report)</b> Unclassified	<b>20. Security Classif. (of this page)</b> Unclassified	<b>21. No. of Pages</b> 31	<b>22. Price</b>

Form DOT F 1700.7 (8-72)

Reproduction of completed page authorized.

## SI\* (MODERN METRIC) CONVERSION FACTORS

### APPROXIMATE CONVERSIONS TO SI UNITS

Symbol	When You Know	Multiply By	To Find	Symbol
<b>LENGTH</b>				
in	inches	25.4	millimeters	mm
ft	feet	0.305	meters	m
yd	yards	0.914	meters	m
mi	miles	1.61	kilometers	km
<b>AREA</b>				
in <sup>2</sup>	square inches	645.2	square millimeters	mm <sup>2</sup>
ft <sup>2</sup>	square feet	0.093	square meters	m <sup>2</sup>
yd <sup>2</sup>	square yard	0.836	square meters	m <sup>2</sup>
ac	acres	0.405	hectares	ha
mi <sup>2</sup>	square miles	2.59	square kilometers	km <sup>2</sup>
<b>VOLUME</b>				
fl oz	fluid ounces	29.57	milliliters	mL
gal	gallons	3.785	liters	L
ft <sup>3</sup>	cubic feet	0.028	cubic meters	m <sup>3</sup>
yd <sup>3</sup>	cubic yards	0.765	cubic meters	m <sup>3</sup>
NOTE: volumes greater than 1000 L shall be shown in m <sup>3</sup>				
<b>MASS</b>				
oz	ounces	28.35	grams	g
lb	pounds	0.454	kilograms	kg
T	short tons (2000 lb)	0.907	megagrams (or "metric ton")	Mg (or "t")
<b>TEMPERATURE (exact degrees)</b>				
°F	Fahrenheit	5 (F-32)/9 or (F-32)/1.8	Celsius	°C
<b>ILLUMINATION</b>				
fc	foot-candles	10.76	lux	lx
fl	foot-Lamberts	3.426	candela/m <sup>2</sup>	cd/m <sup>2</sup>
<b>FORCE and PRESSURE or STRESS</b>				
lbf	poundforce	4.45	newtons	N
lbf/in <sup>2</sup>	poundforce per square inch	6.89	kilopascals	kPa
<b>APPROXIMATE CONVERSIONS FROM SI UNITS</b>				
Symbol	When You Know	Multiply By	To Find	Symbol
<b>LENGTH</b>				
mm	millimeters	0.039	inches	in
m	meters	3.28	feet	ft
m	meters	1.09	yards	yd
km	kilometers	0.621	miles	mi
<b>AREA</b>				
mm <sup>2</sup>	square millimeters	0.0016	square inches	in <sup>2</sup>
m <sup>2</sup>	square meters	10.764	square feet	ft <sup>2</sup>
m <sup>2</sup>	square meters	1.195	square yards	yd <sup>2</sup>
ha	hectares	2.47	acres	ac
km <sup>2</sup>	square kilometers	0.386	square miles	mi <sup>2</sup>
<b>VOLUME</b>				
mL	milliliters	0.034	fluid ounces	fl oz
L	liters	0.264	gallons	gal
m <sup>3</sup>	cubic meters	35.314	cubic feet	ft <sup>3</sup>
m <sup>3</sup>	cubic meters	1.307	cubic yards	yd <sup>3</sup>
<b>MASS</b>				
g	grams	0.035	ounces	oz
kg	kilograms	2.202	pounds	lb
Mg (or "t")	megagrams (or "metric ton")	1.103	short tons (2000 lb)	T
<b>TEMPERATURE (exact degrees)</b>				
°C	Celsius	1.8C+32	Fahrenheit	°F
<b>ILLUMINATION</b>				
lx	lux	0.0929	foot-candles	fc
cd/m <sup>2</sup>	candela/m <sup>2</sup>	0.2919	foot-Lamberts	fl
<b>FORCE and PRESSURE or STRESS</b>				
N	newtons	0.225	poundforce	lbf
kPa	kilopascals	0.145	poundforce per square inch	lbf/in <sup>2</sup>

# TABLE OF CONTENTS

TECHNICAL DOCUMENTATION PAGE .....	ii
TABLE OF CONTENTS.....	iv
LIST OF FIGURES .....	v
LIST OF TABLES .....	vi
ACRONYMS, ABBREVIATIONS, AND SYMBOLS .....	vii
EXECUTIVE SUMMARY .....	viii
1. INTRODUCTION .....	1
2. OBJECTIVES .....	2
3. LITERATURE REVIEW .....	3
4. METHODOLOGY .....	5
4.1. Laboratory Model-Scale Experiments .....	5
4.2. Laboratory Experiments of Soil Hydro-Mechanical Properties .....	6
4.2.1. Soil Shear Strength Test.....	6
4.2.2. Soil Hydraulic Conductivity Test .....	9
4.2.3. Unsaturated Soil Properties Tests .....	10
4.2.4. Soil Shrinkage Tests .....	11
4.3. Numerical Modeling of Highway Embankments .....	14
5. ANALYSIS AND FINDINGS .....	17
5.1. Laboratory Weathering Experiments.....	17
5.2. Soil Hydro-Mechanical Properties.....	18
5.2.1. Soil Shear Strength Properties .....	18
5.2.2. Soil Permeability.....	19
5.2.3. Unsaturated Soil Properties.....	19
5.2.4. Soil Shrinkage Properties.....	21
5.3. Numerical Analyses Results .....	21
6. CONCLUSIONS.....	27
REFERENCES .....	28

## LIST OF FIGURES

Figure 1. Construction of lab-scale specimen holder.....	6
Figure 2. DS test apparatus. ....	7
Figure 3. Triaxial test apparatus.....	8
Figure 4. Modified Bromhead ring shear test apparatus.....	9
Figure 5. Experimental setup for hydraulic conductivity test.....	10
Figure 6. SWRC test setup: (a) Tempe cell apparatus and (b) WP4C apparatus.....	11
Figure 7. Linear shrinkage test setup: (a) before drying and (b) after drying.....	12
Figure 8. Static compaction of volumetric shrinkage samples. ....	12
Figure 9. (a) Stitched pictures of trimmed 4 sides of specimen and (b) threshold of picture.....	13
Figure 10. Texas site slope geometry. ....	14
Figure 11. Texas site observed height of slope failure. ....	15
Figure 12. Time history of volumetric moisture sensors in environmental climate in Baton Rouge, LA. ....	18
Figure 13. Consolidated drained triaxial test of compacted clay from Texas at normal stress of 170 kPa.....	19
Figure 14. (a) SWRC of Texas site as compacted condition and (b) SWRC of Texas site after wet-dry cycles. ....	20
Figure 15. (a) The pore water pressure distribution at the middle of the slope after 1 day of rainfall event and (b) calculated minimum slope FOS.....	22
Figure 16. (a) The pore water pressure distribution at the middle of the slope after 1 day of rainfall event (Case 2) and (b) calculated minimum slope FOS. ....	23
Figure 17. (a) The pore water pressure distribution at the middle of the slope after 10 days of rainfall event (Case 2) and (b) calculated minimum slope FOS.....	24
Figure 18. Observed perched water table during the Texas site visit. ....	25
Figure 19. (a) The pore water pressure distribution at the middle of the slope after 10 days of rainfall event (Case 3) and (b) calculated minimum slope FOS for lime treated slope. ....	26

## **LIST OF TABLES**

Table 1. 10 years return period of precipitation frequency estimates for Denison, TX (54).....	15
Table 2. Calibration of METER sensors.....	17
Table 3. Shear strength parameters of Texas site. ....	18
Table 4. Volumetric shrinkage properties of Texas site soil. ....	21
Table 5. Calculated FOS values after different rainfall amount for Texas site slope. ....	25

## **ACRONYMS, ABBREVIATIONS, AND SYMBOLS**

DOT	Department of Transportation
DS	Direct Shear
FOS	Factor of Safety
FSS	Fully Softened Strength
LSU	Louisiana State University
MDD	Maximum Dry Density
OMC	Optimum Moisture Content
SWRC	Soil Water Retention Curve
UTA	University of Texas at Arlington



## EXECUTIVE SUMMARY

The overarching objective of this research is to develop a framework that can rate and identify areas of high probability of failure of highway embankment slopes. The research project consisted of five tasks to address the aforementioned objective. The first task involved systematically reviewing literature on the effects of long-term cyclic wetting-drying phases on hydro-mechanical properties of clayey soils and comprehending the current state of practice to evaluate the impact of such weathering cycles. The second task involved conducting laboratory model-scale experiments of Louisiana and Texas soils and relate the laboratory test results to weathering cycles by accounting for parameters such as rainfall intensity and duration, evapotranspiration, temperature, and relative humidity. The physical models of the embankments were constructed in the laboratory-controlled environment using the bulk soil samples that were collected from failed embankment sites and were instrumented with soil moisture and temperature sensors. The embankments were exposed to different environmental conditions by using an artificial precipitation system consisting of a grid of perforated PVC piping coupled with an automatic irrigation system. The embedded sensors provided a measure of fluctuations in moisture content and temperature when the embankment models were exposed to fluctuating environmental conditions. The third task involved conducting laboratory testing to determine the strength and unsaturated soil properties of samples collected from laboratory model-scale experiments and to investigate the subsequent changes in the hydro-mechanical properties of those clayey soils. Moreover, newly compacted cylindrical soil specimens were also exposed to wetting and drying cycles prior to testing the hydro-mechanical properties. The properties of unsaturated soils were used to predict soil suction levels of failed embankment slope. Soil Water Retention Curve (SWRC) was used to determine the depth of the moisture fluctuation, which in turn facilitated identification of the zone where the shear strength of clay deteriorated due to the cycles of wetting and drying. Linear and volumetric shrinkage tests were conducted to study the shrinkage characteristics of soil specimens due to loss of moisture. Furthermore, the shrinkage test results provided a measure of the propensity and extent of strength loss incurred by a soil specimen when exposed to weathering cycles. The fourth task involved performing numerical modeling of highway embankments with material properties and test results obtained from Task 3, to investigate the effects of change in hydro-mechanical properties of the soil on the stability of the slopes. The fifth task involved developing a framework that can be used to predict the locations that have a high risk of slope failure in Region 6 and assess the reliability of the proposed model with field verification from documented slope failures. The changes in soil strength and hydraulic conductivity are functions of probability of highway embankment failure, and hence the outcomes of the third and fourth task were used to develop a framework for predicting high-risk zones.

The results and findings of the research suggest that the shear strength of Texas and Louisiana soils starts at peak strength and undergo significant strength loss when exposed to wet-dry weathering cycles over time to attain the Fully Softened Strength (FSS). Moreover, the saturated hydraulic conductivity increases by 2 to 4 orders of magnitude (i.e.,  $10^2$  to  $10^4$  times) due to the wetting and drying cycles. The reduction in soil strength from peak to FSS and an increase in hydraulic conductivity values provide valuable insight into the development of failure conditions in the embankment with time.

## 1. INTRODUCTION

The resilience of transportation infrastructure, particularly the highway embankment, is extremely crucial for the economic growth of the region and daily commuting services. In the United States, especially in Region 6, the highway embankments were mostly constructed using medium to high plasticity clayey soil. These clayey soils undergo significant volumetric changes due to seasonal climatic changes (1–7). In long drought periods, clayey soil tends to shrink whereas, in rainy period it swells significantly (8–11). Hence, these clayey soils experience a significant change in the hydro-mechanical properties over time. As a result, each year several highway embankment slope failures occur that results in constrained mobility services and high maintenance costs (8).

Each repeated weathering (wetting-drying) cycle produces desiccation cracks in the clayey soil that drastically change the soil's hydro-mechanical properties (12–19). The presence of desiccation cracks in a clayey embankment results in exposure of near-surface layers to moisture intrusion during precipitation. Moreover, the increase in soil hydraulic conductivity leads to rapid wetting of clayey soil during rainfall events. Since the moisture content of the cracked clayey soil increases easily, the clayey soil swells, and as a result the shear strength of soil reduces to FSS. This phenomenon causes numerous, shallow slope failures (4 to 8 ft) that are oriented approximately parallel to the surface of the (17, 20–23). Although, it is well known that the detrimental change in the hydro-mechanical properties of the soil cause these failures, knowledge of the time-dependent change in hydro-mechanical properties is still lacking. Such changes in hydro-mechanical properties are influenced by several factors, including climate, extreme weather events, vegetation-soil-water interaction, evapotranspiration, erosion, formation and deepening of cracks from desiccation, and soil clay size-fraction and mineralogy. Therefore, there is a need to understand the effects of wetting and drying cycles on the hydro-mechanical properties of soils. The aim of this research is to develop a methodology and formulate a predictive tool to identify high-risk slopes. The objective was achieved by identifying the soil parameters and environmental factors that affect the performance of newly compacted clayey fill embankments. Laboratory-scale physical models of embankments were exposed to fluctuating environmental conditions prior to testing of hydro-mechanical properties of the soil and numerical modeling was used for calibration and validation.

## 2. OBJECTIVES

The main objective of this study is to develop a framework that can predict the locations which have a high risk of slope failure and demonstrate its applicability in Region 6. To accomplish the proposed objective, the following tasks were conducted:

Task 1 involved a systematic review of literature pertaining to testing of hydro-mechanical properties with variations in environmental conditions. Reviewing prior long-term cyclic weathering experimental studies that investigated changes in hydro-mechanical properties of high plasticity soils provided valuable insight into the state-of-practice for state Department of Transportation (DOT) engineers and practitioners.

Task 2 consisted of performing experiments on embankment materials built in the laboratory with soils collected from failed embankment sites in Louisiana and Texas. The fluctuations in moisture level and temperature in clayey soils when exposed to weathering cycles were studied as a part of this task using data collected from the embedded sensors. The fluctuating environmental conditions experienced by a highway embankment in field were simulated by accounting for several factors such as rainfall intensity and duration, evapotranspiration, temperature, and relative humidity. The obtained data which attribute to the changes in the behavior of compacted clayey soil were used to develop the design guidelines to select shear strength parameters for stability analysis after the soil has experienced seasonal variations involving wetting and drying cycles.

Task 3 encompassed series of laboratory testing of strength and unsaturated soil properties of Louisiana and Texas soils. The impact of wetting and drying cycles on the changes in soil shear strength and unsaturated soil properties were investigated. The extent of decrease in soil strength and increase in hydraulic conductivity were determined to better understand the failure triggering criteria of the surficial slopes of embankments. This information was then incorporated in the numerical models of the highway embankment to study the effect of rainfall events on the stability of highway embankment slopes that incurred degradation of shear strength properties due to exposure to wetting and drying weathering cycles.

Task 4 included numerical analyses of typical highway embankment slopes affected by weathering cycles. The hydro-mechanical properties obtained from laboratory testing of Louisiana and Texas soils in Task 3, before and after exposure to wetting and drying cycles, were used as input parameters for the development of the numerical model of the embankment. The changes in pore water pressure development when exposed to rainfall events of varying duration and intensity, and its impact on the stability of the surficial slopes based on the local meteorological data were assessed using SEEP/W and SLOPE/W modules of GeoStudio.

Task 5 comprised developing a framework that can predict and identify the locations having a high risk of slope failure in Region 6 and assess the reliability of the proposed model with field verification from documented slope failures. The probability of failure of a highway embankment, which is a function of the (1) moisture intrusion in the soil as related to soil suction; (2) time-dependent shear strength loss to FSS; and (3) slope inclination and soil properties were estimated to predict high-risk zones. Task 5 is currently in progress due to the accruing data from the physical model. It is anticipated that this task will be completed during the implementation period.

### 3. LITERATURE REVIEW

Plastic clayey expansive soils are prevalent in many parts of Texas and Louisiana (24, 25). Pavements and slopes constructed using these soils which invariably included high plastic clayey soils that are susceptible to strength loss when exposed to weathering cycles (2, 3, 26–28). Repeated weathering related wetting and drying cycles might create deep desiccation cracking in the plastic clays that expose the soils to significant moisture infiltration from precipitation and related surface runoff conditions (17). Desiccation cracks of depths ranging between 1 and 6 ft may transpire on the slopes and in the unpaved shoulders, particularly those adjacent to travel lanes (26). An increase in the moisture content of the clayey soils due to rainfall events reduces the shear strength of these soils (29). In addition, the moisture movements will increase volume changes in these soils, causing extensive damage to the slopes and pavement infrastructure by inducing high roughness (30). These volume changes and reduced strength issues of subsoils have resulted in numerous pavement failures and highway slope failures (26, 27, 31, 32). Hence, it is of paramount importance to study the changes in the shear strength parameters and hydraulic properties of the geomaterials and assess the stability and serviceability of man-made slopes present in earthen embankment structures such as highway embankments, dams, and levees (17, 33–36).

The slope stability analysis is often performed using peak shear strength parameters estimated by from direct shear or triaxial tests (37, 38). Day (26) performed a back analysis on a slope located in Oceanside, California, that incurred surficial failures in March 1992. The slope stability analysis was performed using the shear strength parameters obtained by extrapolating the triaxial test result, performed at stress conditions higher than that experienced by the shallow surficial soil layers. The analysis yielded a FOS of greater than one (FOS=1.33), suggesting that the slope should not have failed. It was inferred that the shear strength parameters, especially the effective cohesion intercept at low overburden pressure conditions, are usually overestimated when the effective cohesion is extrapolated based on the direct shear or triaxial tests performed at higher stress conditions (20, 26–28). Furthermore, the cyclic wetting and drying cycles reduce the shear strength of the soil to the fully softened shear strength which is characterized by effective strength parameters that are significantly lower than the peak shear strength parameters (39, 40). The increase in destabilizing stresses due to exposure to moisture, coupled with a decrease in resisting shear strength leads to the instability of the surficial slopes (20). The extent of moisture intrusion and strength loss when exposed to wetting and drying cycles depend on the characteristics of the soil and changes in its hydro-mechanical properties (41, 42).

The effects of wetting and drying cycles on the mechanical and hydraulic properties of clayey soils have been studied by several researchers. Benson (43) conducted a study to comprehend the impact of wetting and drying cycles on soil shrinkage strain and hydraulic properties. The results of the study suggest that soils with high clay fraction and high plasticity index are most prone to experience high shrinkage strains. Moreover, the presence of shrinkage cracks results in a significant increase in soil permeability when the soil is compacted wet of optimum moisture content. The permeability value was reported to increase by around 3 orders in magnitude after the first 3 wetting and drying cycles due to high shrinkage. Powrie and Smethurst (44, 45) indicate that vegetation can affect the wetting and drying cycles on clay slopes. Large trees with expansive roots systems induce higher evapotranspiration, causing desiccation cracks and higher permeability values. In contrast, smaller vegetation that consist of shallower roots can maintain the rainfall and evapotranspiration balance throughout the year and reduce the impact of wetting and drying cycles on the soil. Boynton and Daniel (15) studied the effect of confining stress on the

permeability of soil with desiccation cracks. It was found that the cracks in soil start closing with an increase in effective confining pressure after 30 kPa, which ultimately leads to a reduction in permeability. The desiccation cracks also affect the SWRC of soil (46). Benson et al. (46) investigated the change of unsaturated hydraulic properties of cover soils in ten fields in the USA that were exposed to climatic variation for four years. A significant change in air entry value and slope of SWRC of soil has been observed due to the formation of desiccation cracks. Ishimwe (47) performed tests on field-scale compacted clay liners and subjected them to wetting and drying cycles to calculate the field-obtained SWRC and the hydraulic conductivity functions and compare them with their correspondent laboratory values. The laboratory tests were performed from Shelby tube samples extracted after the drying cycle. It was noted that the hydraulic conductivity values from the laboratory samples were higher due to the desiccation cracks that formed during the drying cycle.

The increase in soil permeability due to desiccation cracks causes rapid water infiltration into the soil which makes the soil swell and lose its strength. Skempton (48) performed back analyses of several failed embankment slopes incorporating the effect of fissure formation in clays and found that the shear strength of clay reduces to fully softened strength in this condition. The FSS was observed to be almost same as the peak strength of normally consolidated clays (39). Kayyal and Wright (13) conducted consolidated-undrained triaxial tests on both laboratory compacted samples subjected to wetting and drying cycles and normally consolidated slurry samples of Paris and Beaumont soils. This research showed the similarity between the failure envelopes of slurry samples and the laboratory compacted samples subjected to wetting and drying cycles. Wright et al. (49) conducted a similar study on high plasticity clay of Eagle Ford Shale. Results of this study indicated that the reduction in shear strength of a newly compacted specimen of Eagle Ford Shale, exposed to wetting and drying cycles, was not as significant as that incurred by normally consolidated specimen prepared from a slurry condition. However, in this research, it was realized that the void ratio of normally consolidated specimens was about 1.3 to 1.7 times more than that of the specimens subjected to wetting and drying cycles. Therefore, the authors hypothesized that the high difference in void ratio between the sample of normally consolidated from slurry and newly compacted samples subjected to wetting and drying cycle might be the reason for the observed behavior.

## **4. METHODOLOGY**

The research study aims to assess the long term performance of highway embankments when exposed to wetting and drying weathering cycles and identify the slopes that are under high risk of failure in Region 6. Existing literature on the variation of soil hydro-mechanical properties with environmental conditions was reviewed to guide the physical model-scale experiments of the Texas and Louisiana soils. Two slope failure sites in Texas and Louisiana were identified and bulk soil samples were collected from the slope failure scarp.

Two laboratory embankment models, one with Texas soil and other with Louisiana soil were compacted to build the physical model in the laboratory. The models were subjected to weathering cycles by accounting for the rainfall intensity and duration, evapotranspiration, temperature, relative humidity, and such other factors. The changes in soil strength and hydraulic conductivity properties, when exposed to weathering cycles, were evaluated based on results obtained from laboratory testing of hydro-mechanical properties of the collected soils. By using finite element method based software, SEEP/W and SLOPE/W modules of GeoStudio, the change in pore water pressure development and factor of safety of the embankment slopes were determined. The details of the procedures adopted to perform the physical model and laboratory tests are provided in the following sections.

### **4.1. Laboratory Model-Scale Experiments**

The model-scale experiments are to evaluate the change in hydro-mechanical properties in a climate environment, which is contrast to the extreme of dry and wet cycles in prior research. The method used for physical modelling of highway embankments was to create containers with medium or high plasticity soils in them, compact the soil, and measure the soil properties over time while the specimens are in the outside environment. Each soil type will have two cylindrical containers that are 3 inches in diameter and 12 inches tall (Figure 1). The implementation of this task was divided into subtasks, where the housing containers for the soil samples were first constructed. This included weather-proofing and creating a drainage structure in the containers to ensure a water balance (i.e., flow in = flow out). More specifically, the water balance includes the terms of rainfall, infiltration into the soil, runoff from the surface, and water that percolates through the soil and is charged from the bottom drainage layer. Conserving the water volume will facilitate the numerical modeling. The containers were constructed on 3:1 slopes to better simulate real-world slope angles found on embankments. The next subtask was obtaining soils from Louisiana and Texas slopes. This was completed and the soils are undergoing the process of drying and preparation for compaction. These experiments are considered to be long-term experiments because the change in hydraulic and strength parameters takes to time to occur. Thus, the implementation and data collection of these experiments are still ongoing. Initial results are provided in the

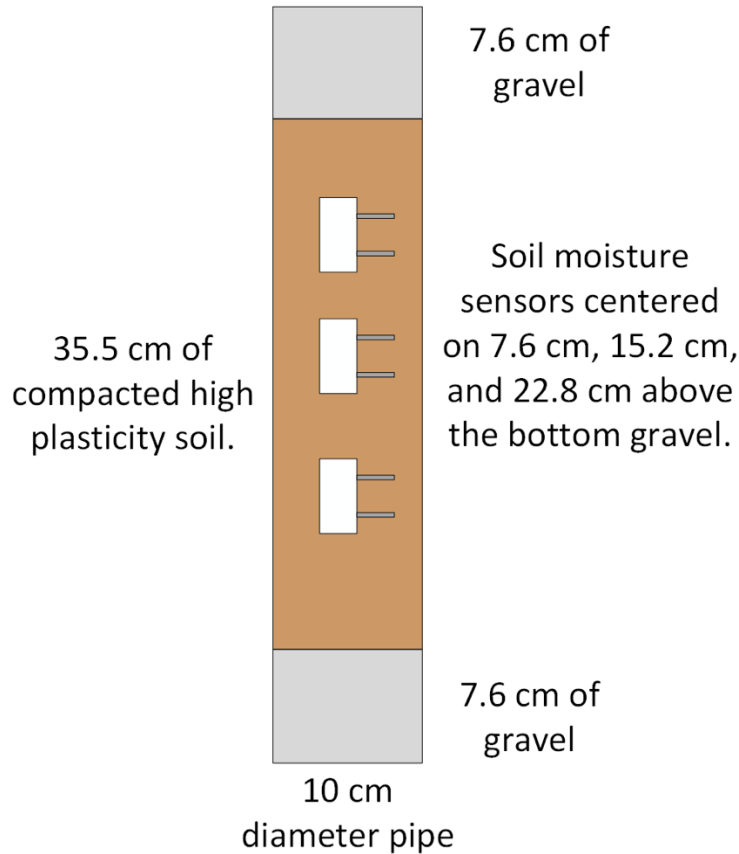


Figure 1. Construction of lab-scale specimen holder.

## 4.2. Laboratory Experiments of Soil Hydro-Mechanical Properties

### 4.2.1. Soil Shear Strength Test

To conduct rainfall-induced slope stability analyses, the shear strength parameters of the soils need to be determined based on the embankment condition that is analyzed. Typically, a highway slope constructed by compacting the clayey soil, has appreciable shear strength, especially cohesion, which can maintain the stability of the slopes. However, these slopes are affected by the formation of desiccation cracks due to the effect of wetting and drying cycles on the surficial area of slopes. The subsequent reduction in shear strength has a detrimental impact on the stability of the slope, especially the surficial region. In this research, the peak shear strength parameters were determined by direct shear (DS) test to assess the shear strength properties of soil prior to experiencing softening behavior (Figure 2). DS tests were conducted as per ASTM D3080, and effective friction angle and cohesion value were estimated. A statically compacted cylindrical specimen of 63.5 mm (2.5 in) diameter and 25.4 mm (1 in) height was used for the DS testing. Tests were conducted under normal stresses of 50, 100, and 150 kPa (1044, 2089, and 3133 psf). The specimen was completely saturated and consolidated at the respective normal stress prior to shearing at a rate of  $4.4 \times 10^{-3}$  mm/m ( $1.73 \times 10^{-4}$  in/min). A slow rate of shearing was used to simulate a drained condition in the specimen and estimate the effective stress parameters. As part of a rehabilitation procedure, lime treated soil was considered in the top layer. Lime treatment leads to a decrease in soil swelling and shrinkage character and improves soil strength parameters. Therefore, the peak

shear strength of 8% lime treated soil samples was determined under the same set of normal stresses on unsaturated conditions after 7 days of curing period.

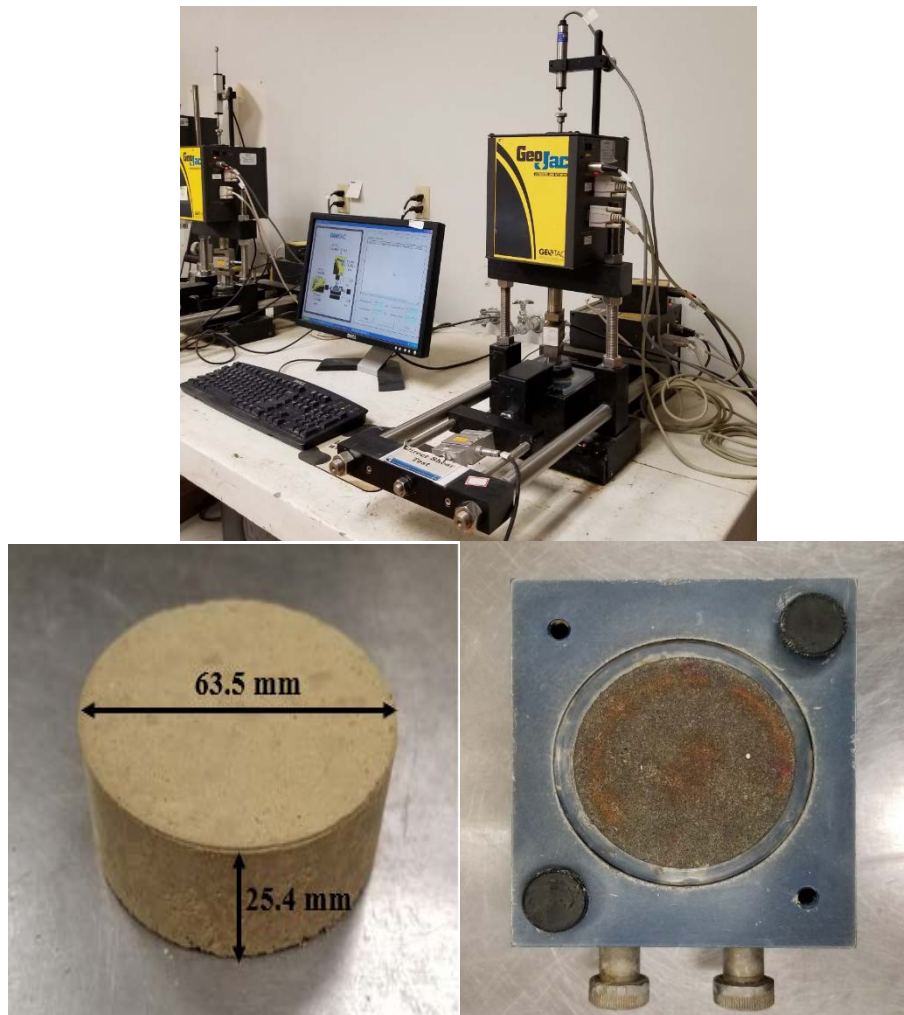
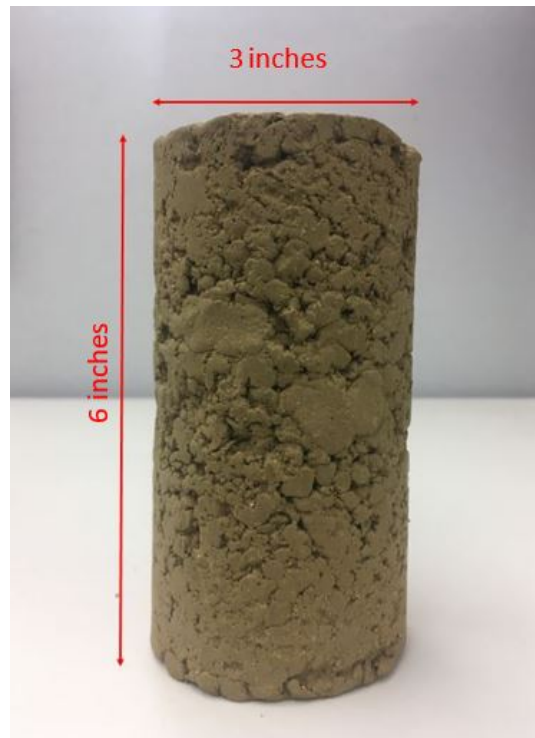


Figure 2. DS test apparatus.

The triaxial shear test is used to determine the drained peak shear strength parameters (Figure 3). In this test, a soil specimen is prepared using dry clay soil and adding water to reach its optimum moisture content, which was 19% based on the results of proctor test. The specimen is encased by a thin rubber membrane and placed inside a plastic cylindrical chamber that is filled with water. The next step is saturating the specimen by pumping water using a GeoJac hydraulic pump (pore pump). The next step is consolidation. In this step the specimen is subjected to an all-around confining pressures 12, 50, and 100 kPa by compression of the water in the chamber using another GeoJac hydraulic pump (cell pump). As confining pressure is applied, at first the pore water pressure of the specimen increases but after a few hours it starts to decrease until reaches zero. After this step the shearing step begins. To cause shear failure in the specimen, axial stress is applied using a GeoJac loading frame. Initial results are provided and subsequent experiments are ongoing with specimen weathering.





**Figure 3. Triaxial test apparatus.**

To determine the shear strength of clay that was exposed to wet-dry cycles and experienced loss of strength, FSS test was conducted in accordance with ASTM (D7608-10) (Figure 4). The shear strength of soil was determined at normal stresses of 50, 100, and 150 kPa (1044, 2089, and 3133 psf). The annular specimen with an inside diameter of 70 mm (2.75 in) and an outside diameter of

100 mm (4 in) was prepared by mixing soil with water to reach a moisture content 1.5 times of its liquid limit, and the slurry was placed in the annular mold of the modified Bromhead ring shear apparatus. The soil specimen was initially consolidated at a normal stress of 6.25 kPa with increment ratio of 1 to reach the respective target normal pressures. At the end of the consolidation process, the soil sample was sheared at a rate of 0.018 mm/min ( $7.05 \times 10^{-4}$  in/min).

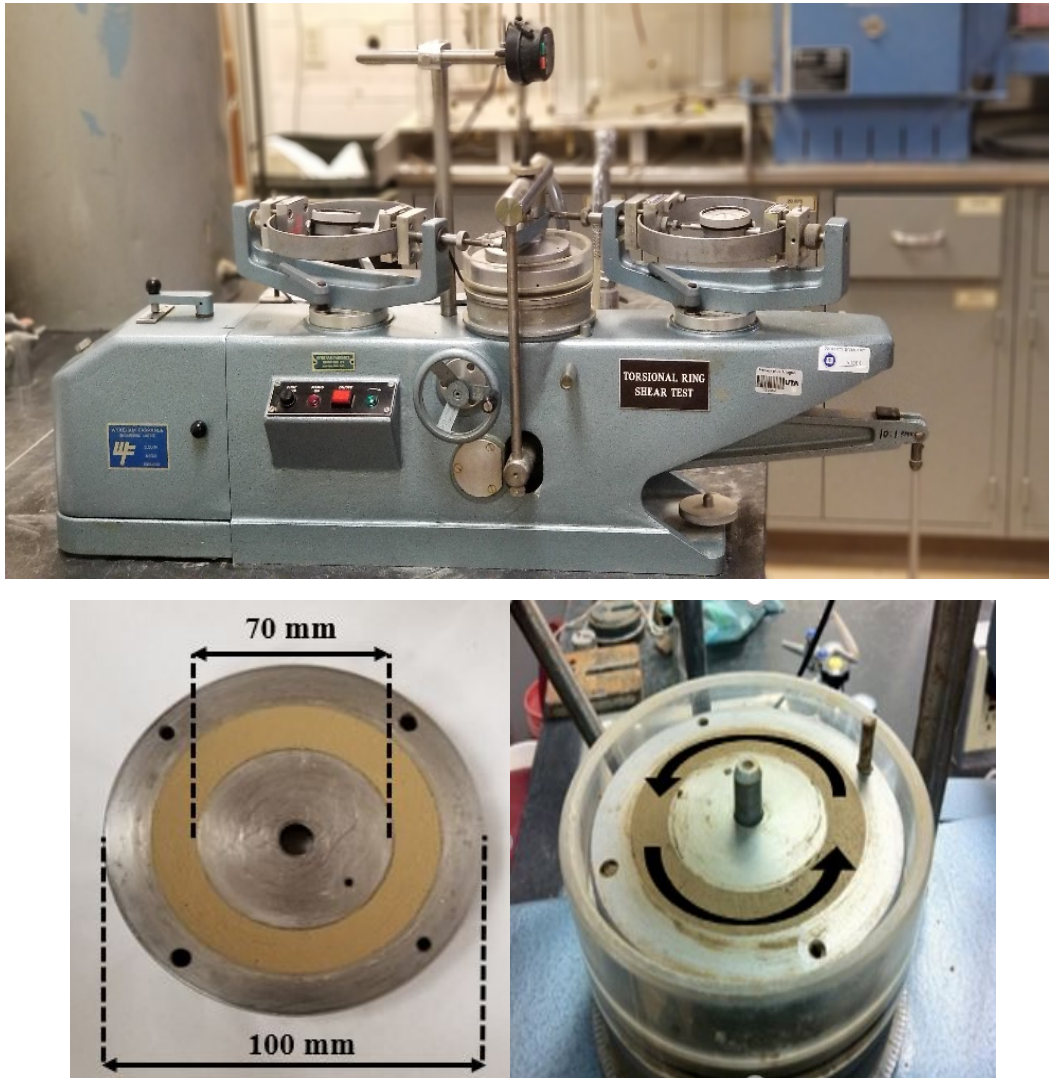


Figure 4. Modified Bromhead ring shear test apparatus.

#### 4.2.2. Soil Hydraulic Conductivity Test

The permeability test of soil was conducted in a flexible wall permeameter as per ASTM D5084-03. The details of the permeameter and its features are provided in Bhaskar et al. (50). The permeability test was conducted to determine the saturated hydraulic conductivity value of a newly compacted clayey soil collected from Texas site. Cylindrical soil specimens of 38.1 mm (1.5 inches) height and 71.12 mm (2.8 inches) diameter were prepared by statically compacting the soil at Optimum Moisture Content (OMC) and 95% of maximum dry density (MDD). The compacted specimen was placed on the base pedestal of permeameter as shown in Figure 5. The sample was saturated using backpressure from the base pedestal. After achieving a  $B$  value of 0.95, the

permeability test was carried out by applying a hydraulic gradient of 35 across the specimen. The rate of inflow and outflow was measured continuously, and the test was stopped when both the rates became equal. The coefficient of permeability was then calculated using Darcy's law.



Figure 5. Experimental setup for hydraulic conductivity test.

#### 4.2.3. Unsaturated Soil Properties Tests

SWRC of a particular soil portrays the relationship between soil suction and moisture content. The SWRC was obtained for newly compacted specimens and specimens exposed to wetting and drying cycles. To determine the unsaturated soil properties, drying path of SWRC test was conducted using Tempe cell and WP4C Dew Point Potentiometer apparatus. Tempe cell apparatus was used for suction levels less than 500 kPa, whereas, WP4C Dew Point Potentiometer apparatus was used for suction values more than 500 kPa. Figure 6 shows the Tempe cell and WP4C Dew Point Potentiometer apparatus used in this research study. Before starting the Tempe cell test, the soil specimen was saturated by submerging in the distilled for approximately 72 hours. The weight of the specimen was checked frequently until there was no appreciable increase in weight.

For all the soil specimens, the tests were started under a near-saturated condition. Different levels of air pressure were applied to the cell, and the water content of the specimens was calculated at every step by recording the amount of water coming out of the sample. The remaining portion of the SWRC corresponding to the relatively high suction range was determined using the WP4C apparatus. The total suction measured using WP4C Potentiometer was assumed to be equal to the soil matric suction due to the absence of appreciable quantity of dissolved salts. An approximate volume of 7 cm<sup>3</sup> soil was placed in the chamber of the WP4C device. After sealing the chamber, the relative humidity above the soil was measured by the WP4C device to provide the suction value at a moisture content. After each step, the moisture content of the soil was varied, and the corresponding suction values were measured. The complete SWRC obtained using the Tempe Cell

and WP4C device was fitted with Van Genuchten best fitting curves (51). The soil matric suction value of soil directly affects the soil strength and unsaturated hydraulic conductivity values. Therefore, the obtained Van Genuchten unsaturated soil parameters were used as input parameters in the numerical analyses.

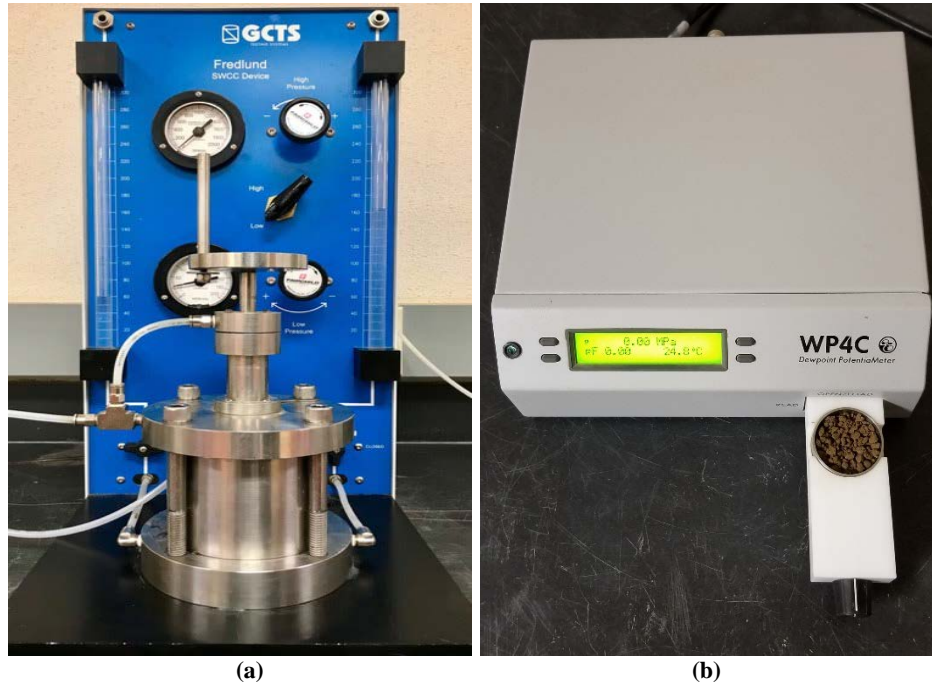


Figure 6. SWRC test setup: (a) Tempe cell apparatus and (b) WP4C apparatus.

#### 4.2.4. Soil Shrinkage Tests

Soils with higher shrinkage potential usually experience more infiltration of moisture during wetting periods, making it imperative to estimate the shrinkage strains of expansive soils. The increase in soil swelling and shrinkage strains eventually lead to a decrease in soil strength and an increase in soil permeability. This phenomenon finally results in instability of the slopes of a highway embankment, leading to surficial failures. The shrinkage properties of soils were determined to estimate the reduction in the volume of soil specimens due to loss of moisture in drought periods by conducting linear shrinkage and volumetric shrinkage test. The linear shrinkage test was conducted as per Tex-107-E which provides the one-dimension linear shrinkage strain by measuring both the length of the wet and dry soil bar. Dry soils were mixed with the required amount of water to attain a target consistency specified in Tex-107-E and molded as shown in Figure 7a. The molds were first kept at room temperature condition until a slight color change and then dried in an oven at 110°C (230°F). The lengths of dried specimens (Figure 7b) were measured by Vernier calipers, and the linear shrinkage was calculated as the percentage reduction in length with respect to the initial length of wet specimens.

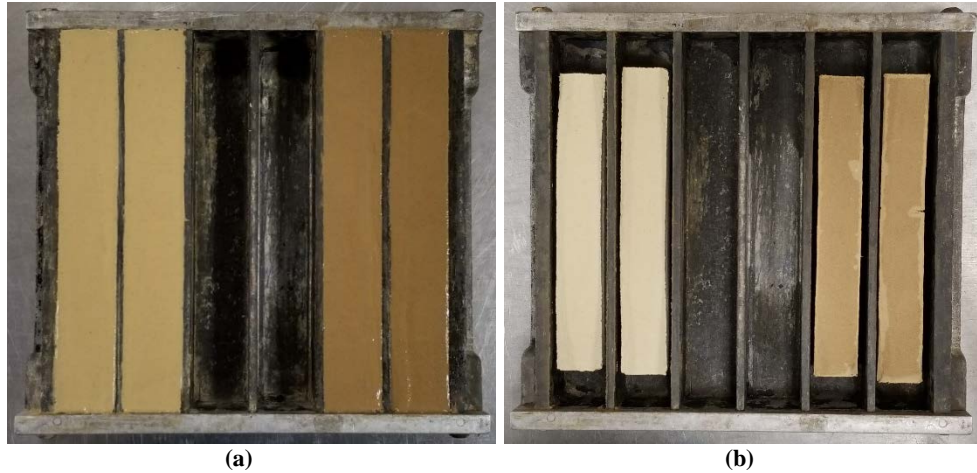


Figure 7. Linear shrinkage test setup: (a) before drying and (b) after drying.

Besides estimating the linear shrinkage strains, the volumetric three-dimension shrinkage properties of the soil were measured using digital imaging technology as per the procedure outlined in Puppala et al. (52). Cylindrical soil specimens of 154.4 mm (6.08 inches) height and 71.12 mm (2.8 inches) diameter were prepared by statically compacting the soil at Optimum Moisture Content (OMC), wet of optimum moisture content, and dry side of optimum moisture content of corresponding to 95% of maximum dry density (MDD) as shown in Figure 8.



Figure 8. Static compaction of volumetric shrinkage samples.

Subsequently samples were cured in the mold at room temperature for twelve hours, after which they were transferred to an oven set at a temperature of 158°F for twenty-four hours. After drying, the camera was placed 50 cm away from the edge of soil samples and a total of 6 pictures (two photographs of the top and base views of the soil sample and four photographs of the surface view with 90° angle apart) were taken immediately. The surface view pictures were cropped and then attached together into one image as presented in Figure 9a. This cropped and attached picture were analyzed with Imagej software. The number of pixels in the pictures were measured and the area of pixels were determined after oven drying. The area of pixel in cracked area of specimens were determined after using the software function of threshold (Figure 9b). The determined area of pixels was deducted from the total area of pixels to estimate the net uncracked area.

The surface area ratio ( $R_s$ ) was determined by dividing the obtained net surface area by the initial unshrunk surface area of the sample soil. The circular cross-sectional area was measured in pixel by averaging from both top and bottom view photographs of the shrunk soil sample. The area ratio ( $R_c$ ) in the analysis is obtained by taking the ratio of pixel area from the average cross-sectional area and the initial cross section area of the dummy cylinder. The perimeter ratio ( $R_p$ ) in the analysis was obtained by taking the initial and shrunk diameters of the soil specimen were calculated from the circular area. Finally, the volumetric shrinkage (VS) determined using the following equation.

$$VS = 1 - \left( \frac{R_s \times R_c}{R_p} \right) \times 100 \quad [1]$$

where:

VS= Volumetric shrinkage (%);

$R_s$  = Surface area ratio;

$R_c$  = Cross-section area ratio; and

$R_p$  = Perimeter ratio.

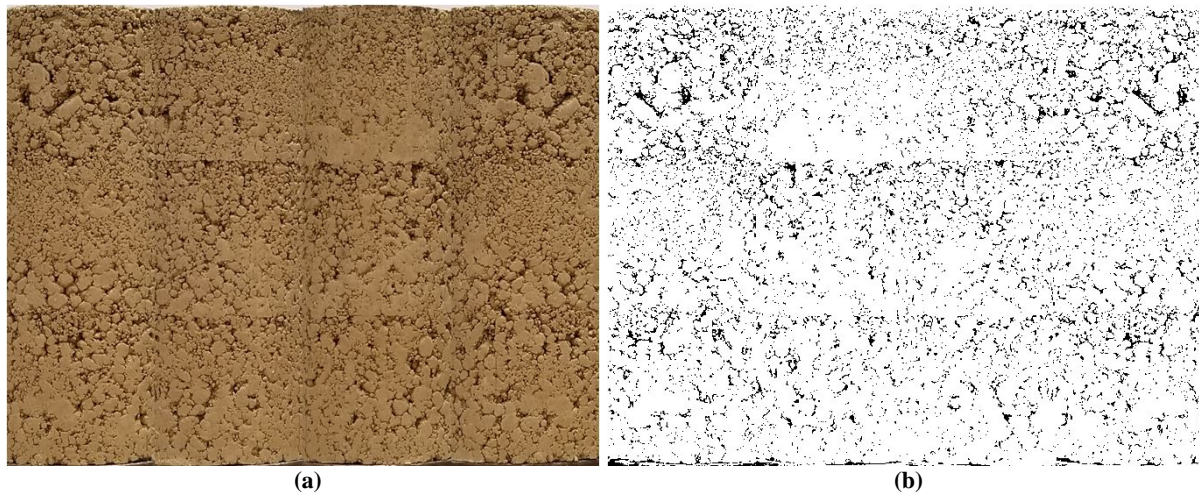


Figure 9. (a) Stitched pictures of trimmed 4 sides of specimen and (b) threshold of picture.

### 4.3. Numerical Modeling of Highway Embankments

To demonstrate the effects of wetting and drying weathering cycles on the stability of highway embankments built with clayey soils, rainfall-induced slope stability issues were analyzed for Texas site slope by using SEEP/W and Slope/W modules of GeoStudio. Highway embankment slopes are mostly present in an unsaturated condition where the soil suction contributes towards the shear strength of the soil. However, infiltration of rainwater increases the water content and degree of saturation of the soils that were in an unsaturated condition prior to a rainfall event. The distribution of water content is affected by such rainfall events, consequently affecting the stability of the slope. In order to capture this phenomenon, a transient seepage analysis was conducted at first by using SEEP/W.

The geometry of the embankment slope located at Texas site was obtained from the as-built drawing provided by local DOT (Figure 10). The original slope had a height of 10.6 m (34.8 ft) with a slope of 3:1 horizontal to vertical. The post-failure depth was observed to be approximately 2.13 m (7ft), measured perpendicular to the slope (Figure 11). The plane strain model of the slope was built with soil layers having two different material properties (1) surficial layer that was exposed to wetting and drying cycles within 2.13 m (7ft) from the surface and (2) deeper layer that was not affected by weathering cycles (Figure 10).

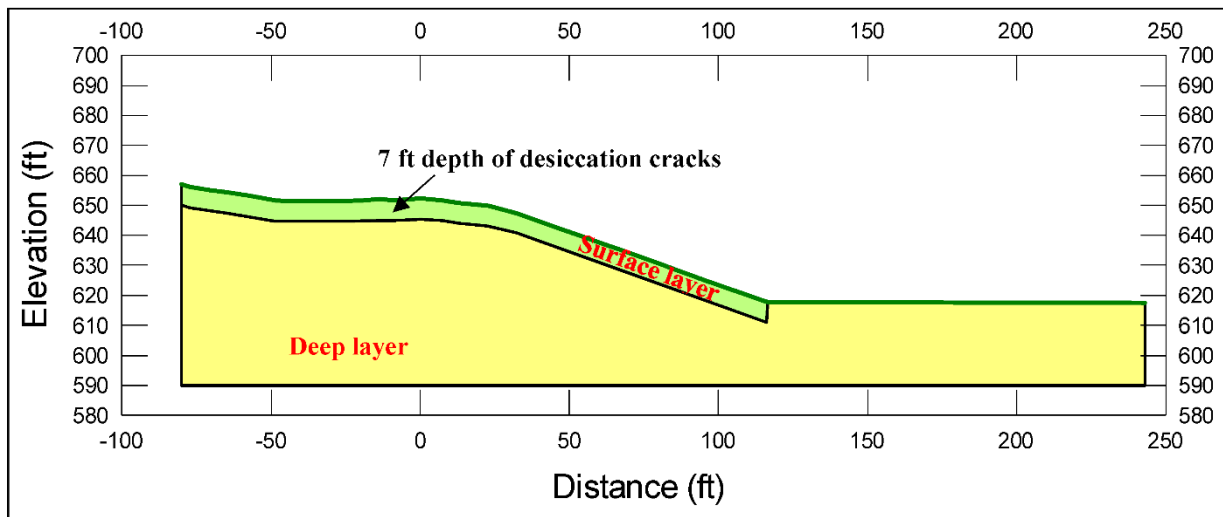


Figure 10. Texas site slope geometry.



Figure 11. Texas site observed height of slope failure.

The initial conditions play a critical role in the transient seepage analysis results since soil strength and rate of infiltration depend on initial soil suction levels. In situ testing results suggested absence of water table above the 590 ft elevation. Therefore, the water table was assigned at an elevation of 590 ft in the numerical model of the embankment. The matric suction was estimated as the product of height above water table and unit weight of water. However, this approximation resulted in high suction level near the crest of slope (about 200 kPa). To prevent such high value of suction and its corresponding contribution towards shear strength, the initial suction level was limited to a maximum value of 50 kPa, which is similar to the approximation made by Lee et al. (53). The cut-off value of matric suction (i.e., 50 kPa) was decided based on the water content of samples collected from the site and estimating the corresponding matric suction values from the SWRC.

For Texas site, the exact date of slope failure and conditions that lead to the failure were not known to researchers at University of Texas at Arlington (UTA). To assess the effect of rainfall intensity and duration of rain on highway slope factor of safety (FOS), the precipitation frequency estimates provided by the National Oceanic and Atmospheric Administration Atlas 14 (54) were used. This compiled data is based on frequency analyses of partial duration series for selected duration of 1, 4 and 10 days with an average recurrence interval of 10-year period. The induced precipitation duration, the total amount of rainfall and rainfall intensities are presented in Table 1.

Table 1. 10 years return period of precipitation frequency estimates for Denison, TX (54).

Rainfall Duration (Days)	Total amount of rainfall (Inches)	Rainfall intensities (Inches/s)
1	6.21	$7.19 \times 10^{-5}$
4	8.22	$2.38 \times 10^{-5}$
10	10.10	$1.17 \times 10^{-5}$



After conducting transient seepage analyses, the slope model was transferred to SLOPE/W for estimation of the FOS of the slope. Slope stability analyses were performed considering the effect of unsaturated condition of the soil. Unsaturated friction angle of soil,  $\phi_b$ , was assumed to be  $15^\circ$ , based on the recommendations from the existing literature (55). The slope stability analyses were conducted using the Morgenstern-Price method, and the critical slip surface was determined by defining the probable zones of entry and exit of the trial slip surfaces.

The numerical analyses were performed for three different scenarios: (1) Case 1, representing slope stability analysis under short-term condition in which slope did not experience a significant number of weathering cycles, and (2) Case 2, portraying slope stability analysis under long-term condition where the surficial slope experienced desiccation cracking and degradation of hydro-mechanical properties due to exposure to significant number of weathering cycles, and (3) Case 3, representing the slope stability after rehabilitation of slope using 8% lime within 2 feet depth from the surface layer of slope. Peak shear strength parameters of the soil estimated using DS test and saturated permeability values of newly compacted clay samples were assigned to all region of slope model for Case 1 analysis. In Case 2 analysis, the surficial soil layer was assigned with FSS parameters of soil determined using the modified Bromhead ring shear equipment in accordance with ASTM (D7608-10) and permeability value was increased by four orders (i.e.,  $10^4$  times) as compared to that used in Case 1. In Case 3 analysis, in the lime treated layer and overlain untreated layer the peak shear strength parameters obtained during DS tests were assigned to the corresponding region of the slope model.

## 5. ANALYSIS AND FINDINGS

### 5.1. Laboratory Weathering Experiments

The laboratory model first required calibration of the moisture sensors. Six (6) METER TEROS 10 soil moisture sensors that measure the volumetric water content ( $m^3/m^3$ ) and temperature were implemented. Table 2 shows the calibration of the moisture sensors in air, sand and water. In air, the sensors read slightly negative values. In sand, the sensors measure from 0.3 to 0.4 while they measure approximately 0.6 in water. The calibrated sensors are inserted into the boxes for measuring soil moisture.

**Table 2. Calibration of METER sensors**

Port 1	Port 2	Port 3	Port 4	Port 5	Port 6	Measurement
TEROS 10 Soil Moisture	TEROS 10 Soil Moisture	TEROS 10 Soil Moisture	TEROS 10 Soil Moisture	TEROS 10 Soil Moisture	TEROS 10 Soil Moisture	Material
$m^3/m^3$	$m^3/m^3$	$m^3/m^3$	$m^3/m^3$	$m^3/m^3$	$m^3/m^3$	
-0.046	-0.051	-0.052	-0.055	-0.048	-0.061	Air
-0.044	-0.049	-0.055	-0.055	-0.049	-0.062	Air
0.113	0.110	0.107	0.104	0.119	0.096	
0.622	0.669	0.593	0.587	0.635	0.562	Water
0.649	0.675	0.591	0.586	0.676	0.562	Water
0.631	0.675	0.589	0.585	0.670	0.562	Water
0.641	0.676	0.589	0.584	0.691	0.563	Water
0.666	0.592	0.589	0.585	0.689	0.563	Water
0.546	0.410	0.395	0.573	0.621	0.564	
0.320	0.310	0.633	0.527	0.550	0.568	1,2 Sand 3,4,5,6 Water
0.320	0.310	0.634	0.526	0.527	0.568	1,2 Sand 3,4,5,6 Water
0.440	0.427	0.395	0.370	0.575	0.575	3,4 Sand 1,2,5,6 Water
0.560	0.559	0.301	0.300	0.555	0.573	3,4 Sand 1,2,5,6 Water
0.561	0.537	0.301	0.300	0.555	0.574	3,4 Sand 1,2,5,6 Water
0.579	0.535	0.450	0.433	0.379	0.387	5,6 Sand 1,2,3,4 Water
0.592	0.545	0.659	0.570	0.304	0.307	5,6 Sand 1,2,3,4 Water

The soil sensors will be used to be understand the infiltration of rainfall into the soil. As data is accruing in the long-term experiments (Figure 12) changes in soil moisture with time based on the rainfall duration and intensity will facilitate the HYDRUS simulations, which give information on how the unsaturated soil properties change over time. Figure 12 shows the temporal change in volumetric moisture content with time. It is evident that sensor S1 near the surface saturates within 72 hours whereas it takes 12 days for sensor S2 to saturate. Sensor S3 remained unsaturated when the water levels decreased and drying occurred. An axisymmetric HYDRUS model is currently constructed with no flow boundaries along the sidewalls and bottom floor. The top of the model is set to the weather data collected from the Louisiana State University (LSU) Ben Hur weather station. The soil layers are pea gravel overlying 35.5 cm of compacted clay overlaying a pea gravel layer for drainage. A geotextile separated the compacted clay from the pea gravel. At the bottom of the containers is a drainage outlet for water to flow out. The model predictions in soil moisture and volume leaving the system will be compared to the physical experiment. With the calibrated model, further sensitivity simulations can be performed to understand changes in the unsaturated properties with cyclic wetting and drying.

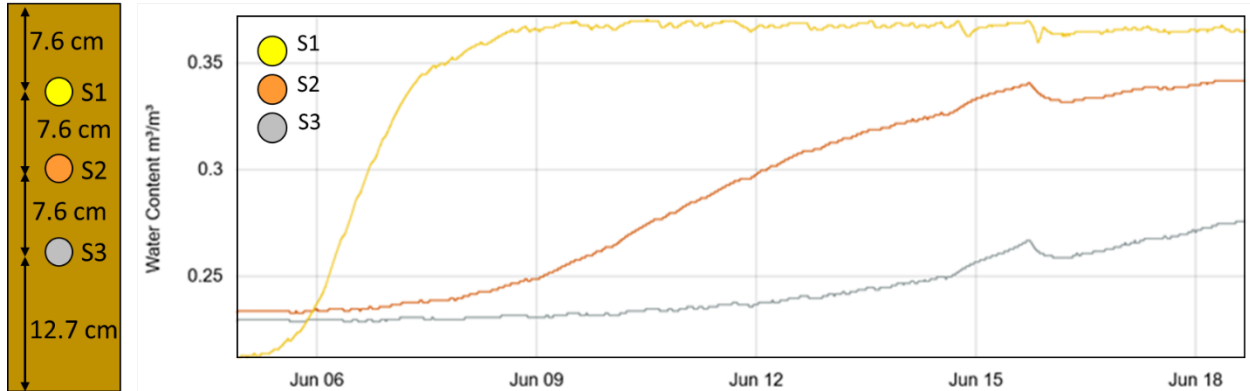


Figure 12. Time history of volumetric moisture sensors in environmental climate in Baton Rouge, LA.

## 5.2. Soil Hydro-Mechanical Properties

### 5.2.1. Soil Shear Strength Properties

Table 3 presents the peak and fully softened strength soil parameters of Texas site. The results suggest that a newly compacted specimen of clayey soil has sufficient cohesion value (13.2 kPa) whereas, in fully softened condition, clayey soil significantly lost its cohesion (reduced to 1.28 kPa). However, the friction angle value was not significantly affected in the fully softened state. Rehabilitation of clayey soil by using 8% lime increased the soil strength parameters significantly. Lime treatment increased soil cohesion value from 13.20 kPa to 173.32 kPa while the friction angle value increased from 23.4° to 43.1°. The estimated data were used as input parameters into the respective regions for the slope stability analysis.

Table 3. Shear strength parameters of Texas site.

Slope region	Strength Type	c' (kPa)	$\phi'$ (degree)
Surficial layer	Peak shear	13.20	23.4
Deep layer	Fully softened	1.28	23.7
Lime treated layer	Peak shear	173.32	43.1

Figure 13 shows the consolidated drained triaxial compression test conducted with a cell pressure of 3,550 psf (170 kPa). The sample size was 3 inches in diameter and 6 inches in height. The reported deviator stress was 22.2 psi (3195 psf, 153 kPa). As multiple specimens are tested, the change from peak shear strength to fully softened will be determined using a regression analysis.

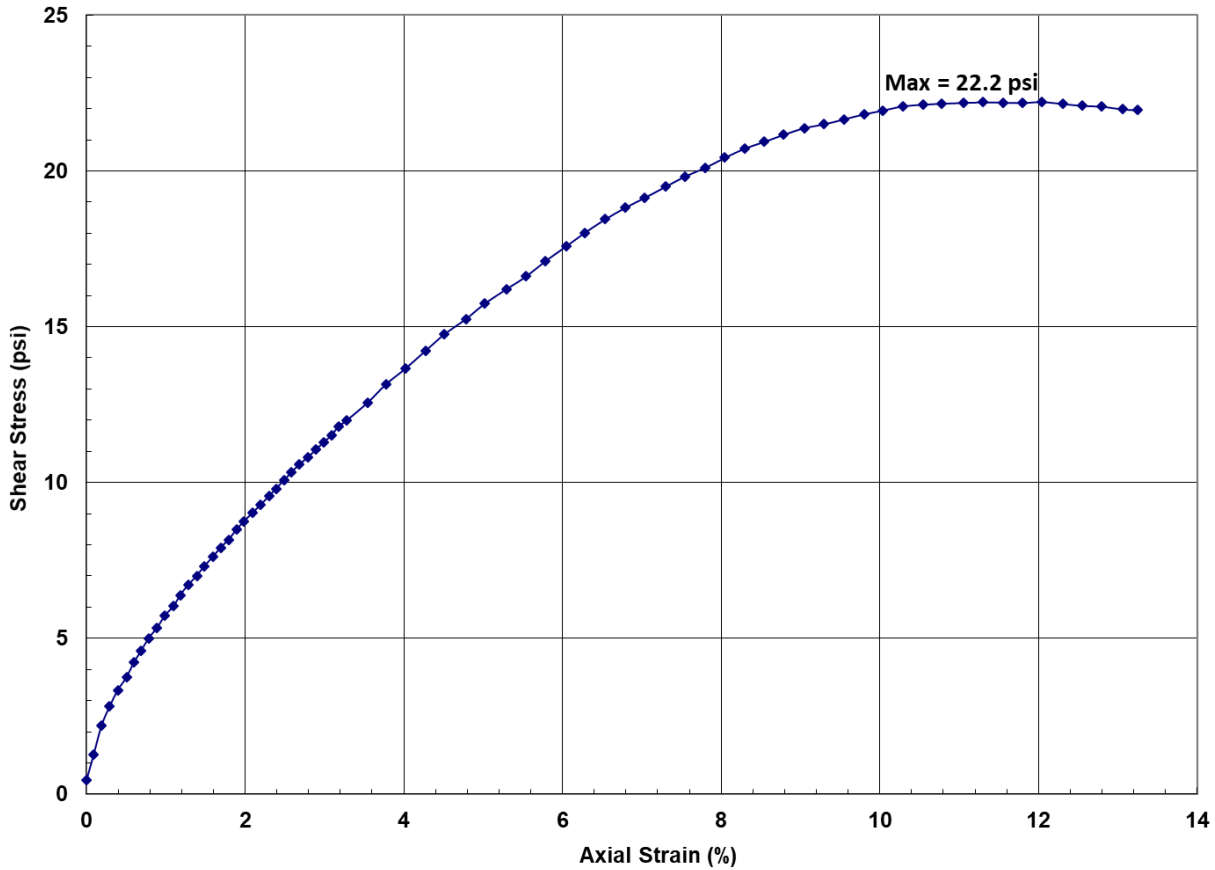


Figure 13. Consolidated drained triaxial test of compacted clay from Texas at normal stress of 170 kPa.

### 5.2.2. Soil Permeability

The hydraulic conductivity was estimated to be  $2.68 \times 10^{-10}$  m/s ( $8.8 \times 10^{-10}$  ft/s) for a newly compacted specimen. Several researchers have reported that the hydraulic conductivity values of clayey soils increase by 2 to 4 orders of magnitude (i.e., increase in  $10^2$  to  $10^4$  times) due to exposure to wetting and drying cycles (14, 56). Therefore, the slope stability analysis for Case 2 was performed for Texas site soil with an increased hydraulic conductivity value of  $2.68 \times 10^{-6}$  m/s ( $8.8 \times 10^{-6}$  ft/s).

### 5.2.3. Unsaturated Soil Properties

The SWRC parameters directly affect the soil moisture distribution changes during rainfall events (54). Therefore, ignoring the changes in SWRC parameters may lead to errors in transient seepage analyses results. The SWRC data and the Van Genuchten best fitting parameters for Texas soil, before and after exposure to wetting-drying cycles are presented in Figures 14a and 14b, respectively. A drastic change in unsaturated soil properties due to exposure to wet and dry cycles was observed. Figure 14b shows that exposure to wetting-drying cycles shifted the SWRC of Texas site soil to the left, resulting in a decrease in the air entry value from 65 kPa (9.43 psi) to 24 kPa (3.48 psi). Furthermore, the Van Genuchten best fitting parameter  $\alpha$  increased 2.1 times from  $0.01 \text{ kPa}^{-1}$  to  $0.021 \text{ kPa}^{-1}$ , and the  $n$  parameter decreased from 2.89 to 1.35. The increase in  $\alpha$  value shifted the SWRC towards the left, resulting in a lower matric suction at a given volumetric water

content. Therefore, it can be concluded that surficial soils exposed to wetting-drying cycles will have a lower contribution of suction-induced shear strength towards the overall shear strength of the soil. The obtained SWRC parameters were used as input parameters in the numerical models to better simulate the long-term performance of slopes exposed to weathering cycles under rainfall condition.

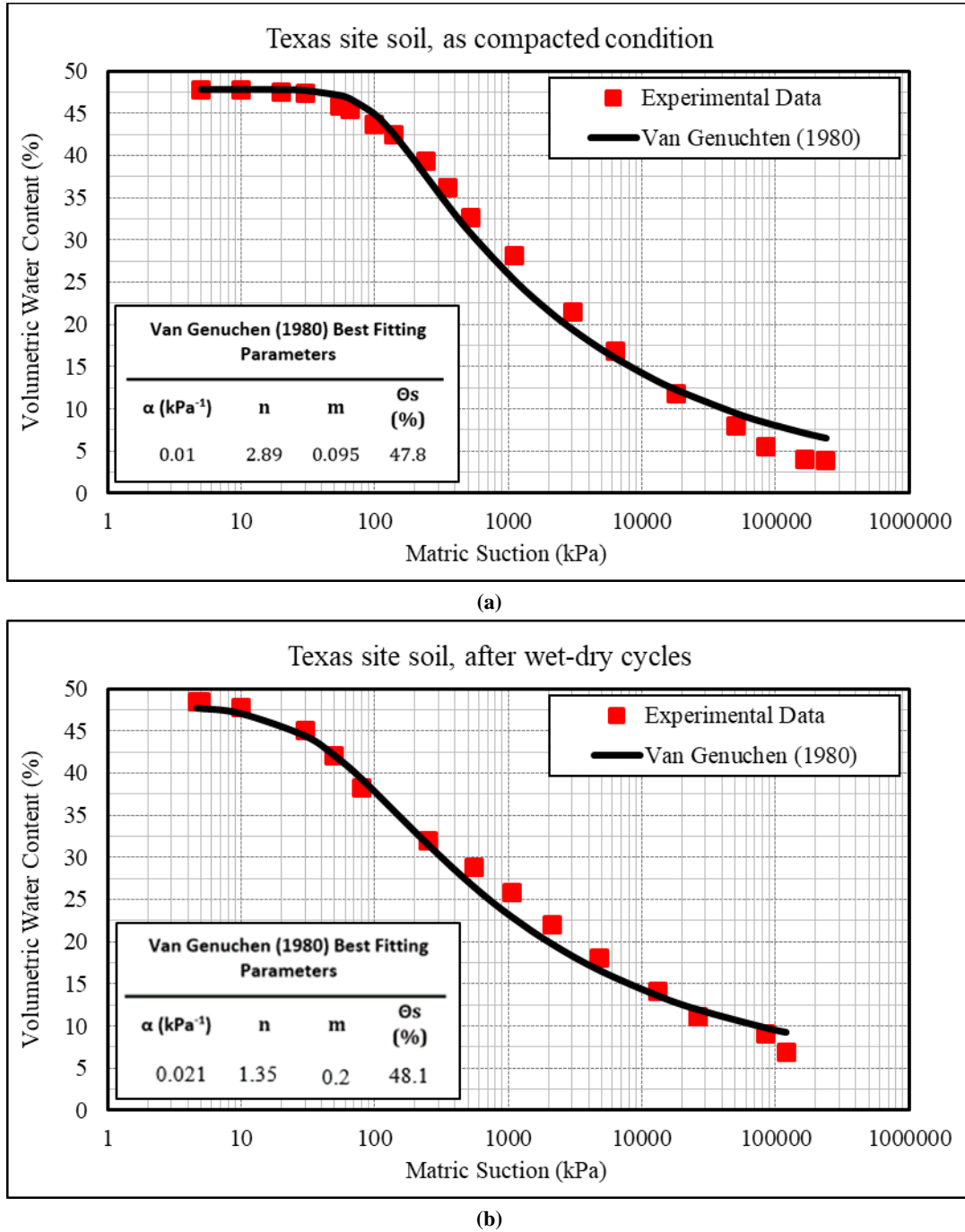


Figure 14. (a) SWRC of Texas site as compacted condition and (b) SWRC of Texas site after wet-dry cycles.

#### 5.2.4. Soil Shrinkage Properties

The linear and volumetric shrinkage strain values of Texas site soil was estimated, and the volumetric shrinkage results are presented in Table 4. Texas soil experienced 17.2% linear shrinkage whereas volumetric shrinkage results are varying between 17.1 to 22.8% with respect to compacted water content. The results show that the soils collected from Texas site experienced significant amounts of shrinkage with both two different tests, a typical property of expansive soils. A higher volumetric shrinkage causes more moisture infiltration during the wetting period after the drought, and it indicates a higher chance of getting drastically affected by shrinking and swelling phenomenon. This may subsequently contribute to the loss of cohesion, an increase in hydraulic conductivity values and eventually lead to failure of surficial slopes of the highway embankment.

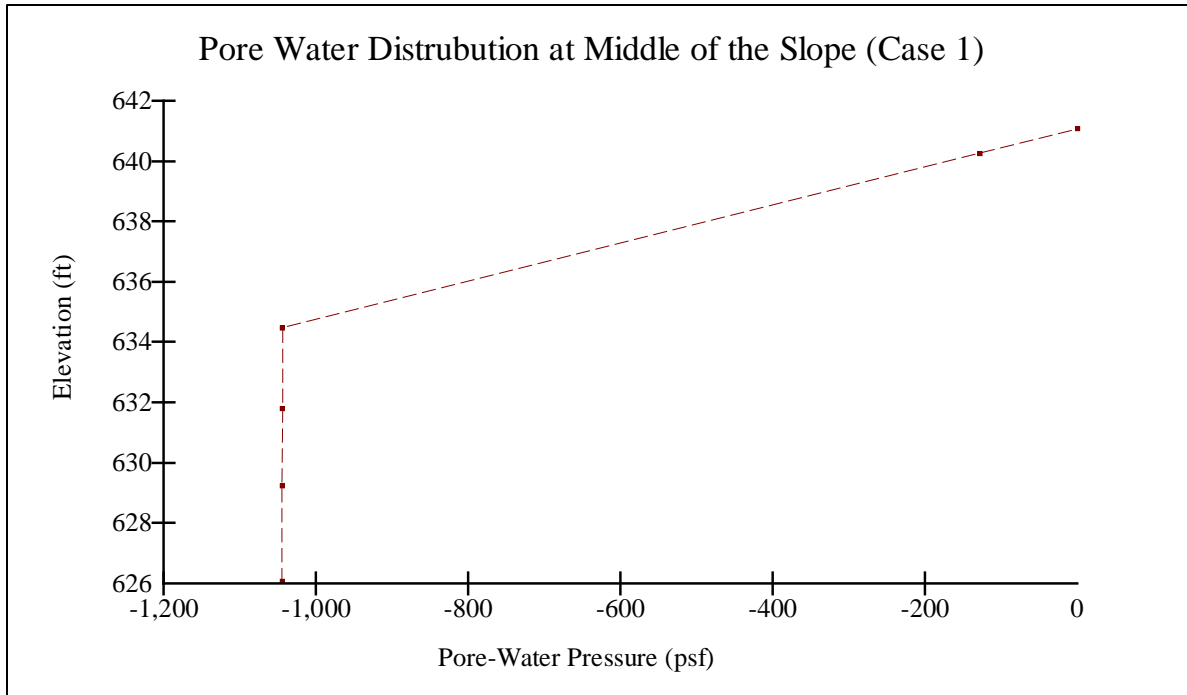
**Table 4. Volumetric shrinkage properties of Texas site soil.**

Compacted water content (%)	Volumetric Shrinkage (%)
17.5 (dry of OMC)	17.1
19.5 (OMC)	19.0
21.5 (wet of OMC)	22.8

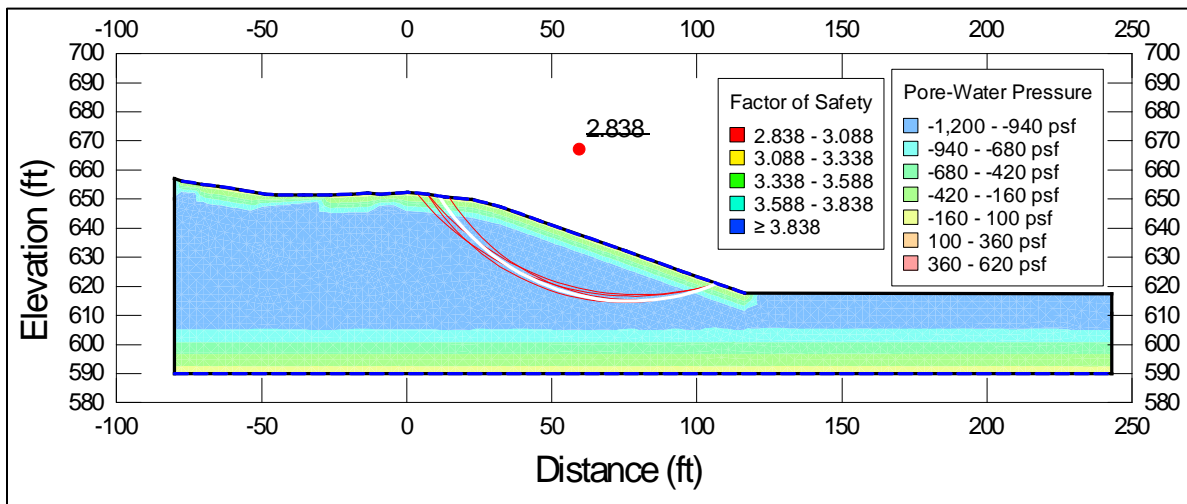
### 5.3. Numerical Analyses Results

Transient seepage and unsaturated slope stability analyses were conducted on Texas site slope by using SEEP/W and SLOPE/W. The respective hydro-mechanical material properties obtained from laboratory testing were used as input parameters to model the behavior of the embankment slope under the two different scenarios. A total of 12 transient seepage and slope stability analyses were conducted to demonstrate the effects of rainfall event on the stability of highway embankments. The FOS of the slopes were calculated for post-construction condition (Case 1), and long-term condition (Case 2) incorporating the effect of desiccation cracks formed along the slope surface layer when exposed to wetting and drying cycles, and (Case 3) considering a lime treated top layer (8% lime).

In Case 1, the newly compacted highway slope had a high FOS value about 2.83, for all the three rainfall events. This can be attributed to the low value of permeability which prevented the percolation of rainwater and presence of high soil shear strength parameter, particularly cohesion. Figure 15a represents the pore water pressure distribution at the middle of the slope after 1 day of rainfall event between the elevations 641 ft to 626 ft. For all the cases, no moisture fluctuation was observed below elevation of 626 ft due to rainfall. The matric suction value decreased from elevation 641 ft to elevation 634.5 ft (6.5 ft) due to an increase in moisture content during rainfall events. Figure 15b shows the minimum FOS of slope (2.83) and the location of the critical slip surface at the end of the rainfall event. The effects of higher air entry value and lower unsaturated hydraulic conductivity value of newly compacted clayey soil prevents the development of deep wetting fronts, leading to a higher FOS of the slope.



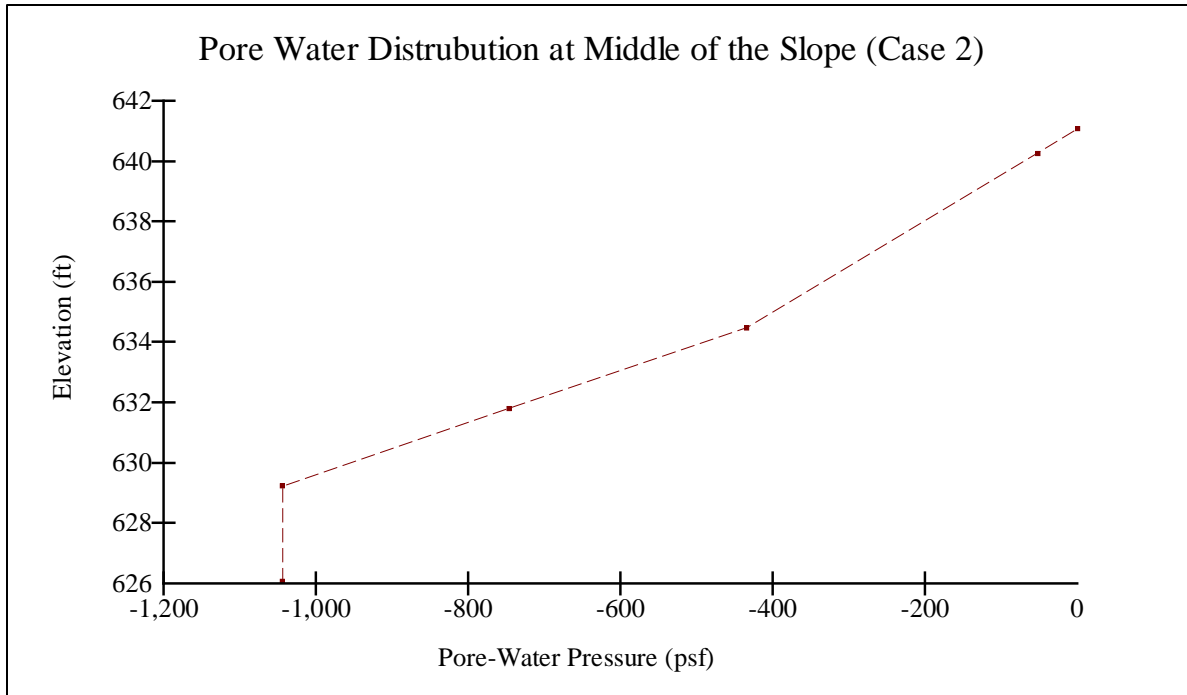
(a)



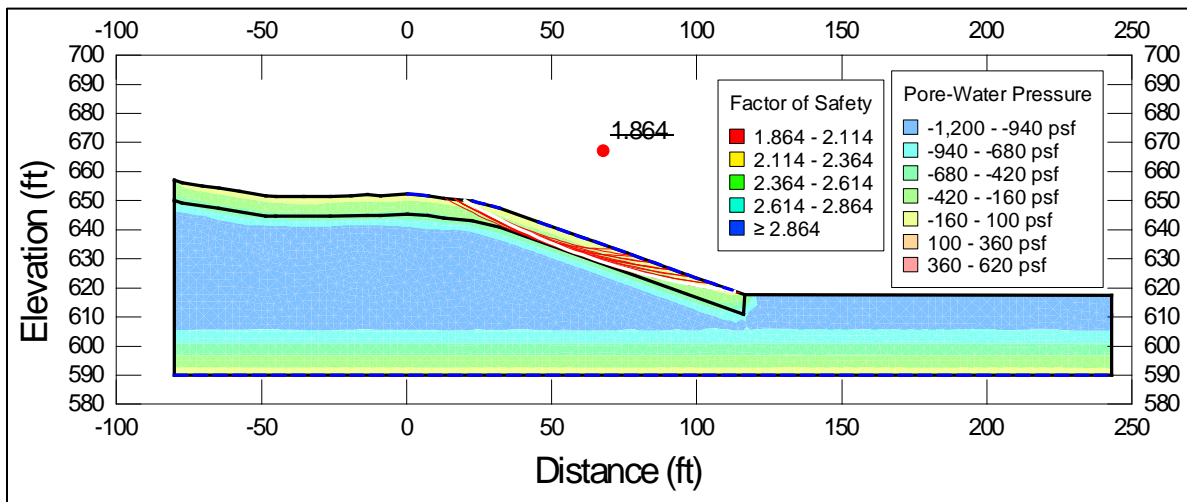
(b)

Figure 15. (a) The pore water pressure distribution at the middle of the slope after 1 day of rainfall event and (b) calculated minimum slope FOS.

Figure 16a presents the pore water pressure distribution at the middle of the slope after 1 day of rainfall event for Case 2 and Figure 16b indicates the calculated minimum FOS of slip surface and its location at the end of the rainfall event. The soil moisture fluctuation can be observed from elevation of 641 ft to 629.2 ft. A drastic change in soil hydraulic properties eventually led to decrease in FOS of slope from 2.839 to 1.864. Unlike Case 1 analysis which exhibited a deep slip surface, the critical slip surface in the Case 2 analysis was surficial in nature, passing through the surficial soil layer which was affected by the wetting and drying cycles.



(a)



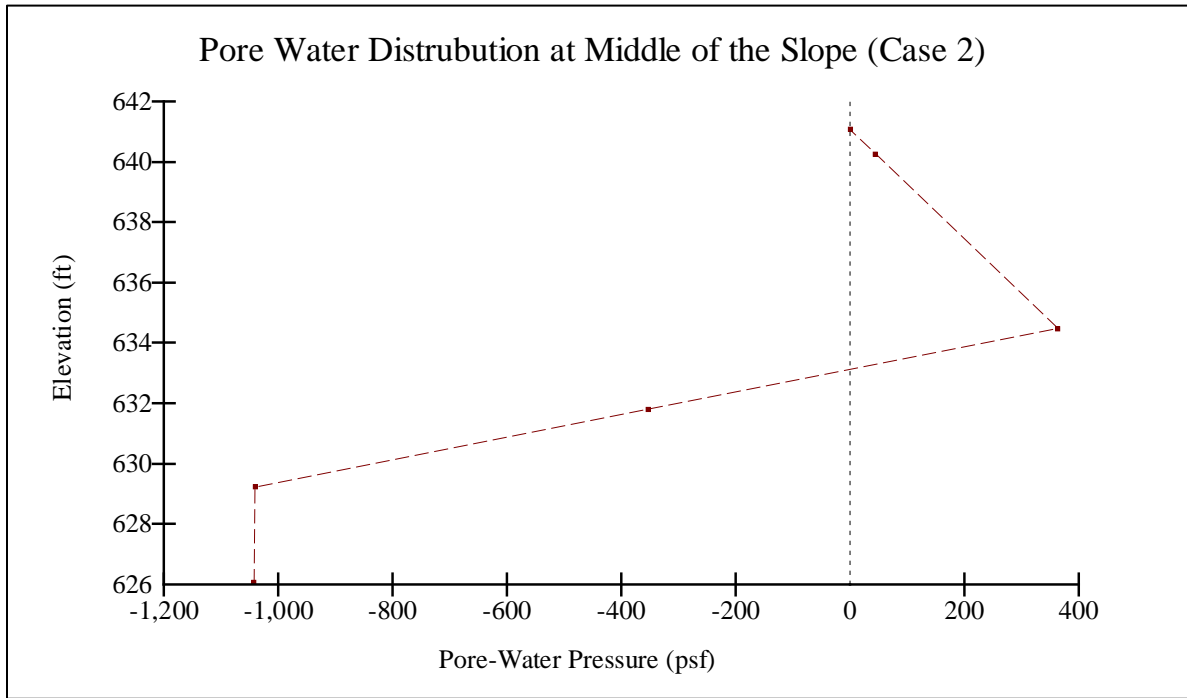
(b)

Figure 16. (a) The pore water pressure distribution at the middle of the slope after 1 day of rainfall event (Case 2) and (b) calculated minimum slope FOS.

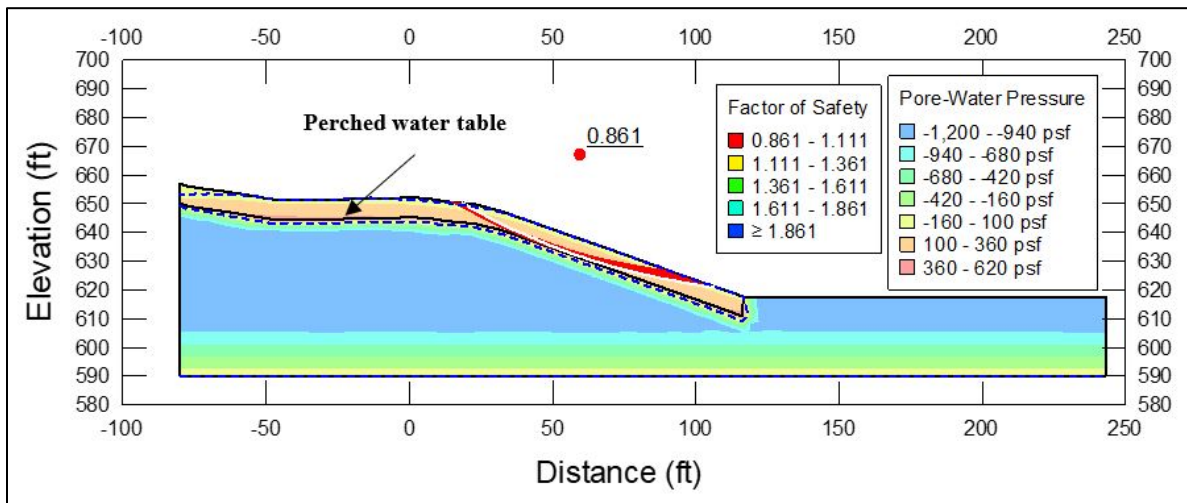
The FOS of slope for Case 2 dropped below one during an analysis performed with 10 days of rainfall infiltration. Figure 17a represents the pore water pressure distribution at the middle of the slope after 10 days of rainfall event for Case 2, and Figure 17b shows the calculated minimum FOS of slip surface along with its location. The positive pore water pressure in the surficial layer between elevations of 641 ft to 633.13 ft reduced the effective soil shear strength, resulting in instability of the slope (FOS < 1). The presence of an underlying layer of low permeability, coupled with a rainfall event with higher intensity and duration, caused the infiltrated water to accumulate and form a saturated zone in the surficial layer. This observed perched water zone from the



numerical analysis (Figure 17b) was consistent with the site visit observations. Figure 18 shows the perched water table observed at a depth of 2 ft below the surface during the site visit.



(a)



(b)

Figure 17. (a) The pore water pressure distribution at the middle of the slope after 10 days of rainfall event (Case 2) and (b) calculated minimum slope FOS.



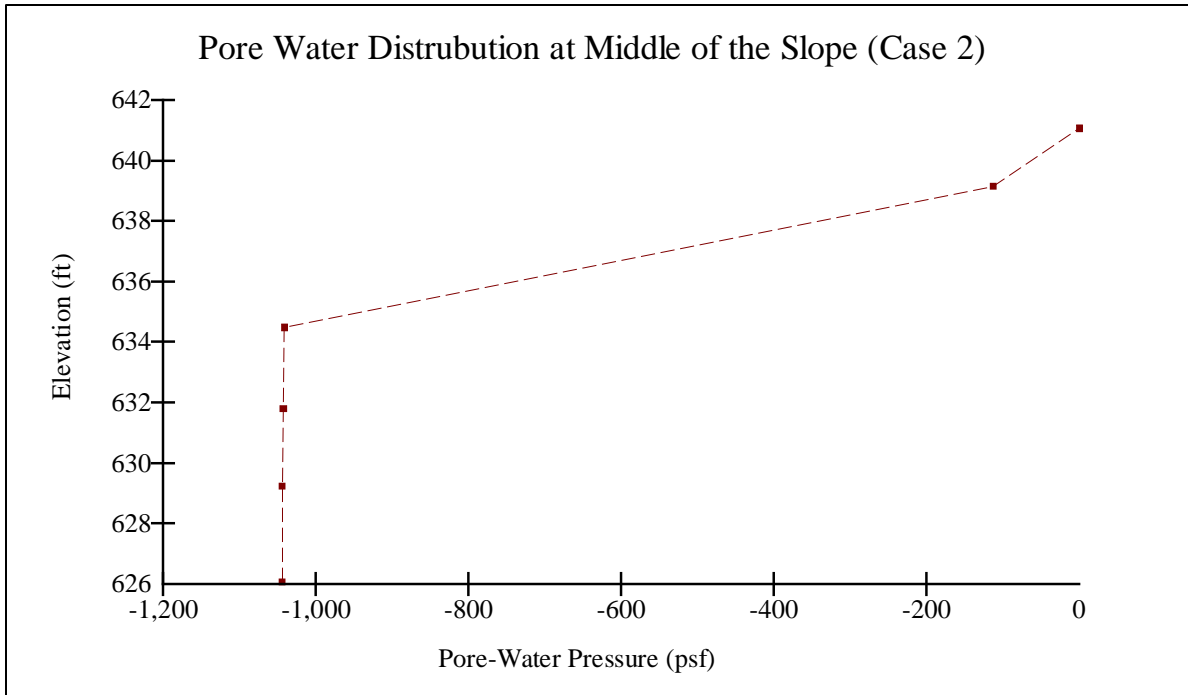
**Figure 18. Observed perched water table during the Texas site visit.**

Figure 19a illustrates the pore water pressure distribution at the middle of the slope after 10 days of rainfall event for case 3 and Figure 19b represents the calculated minimum FOS of slip surface and its location at the end of the rainfall event. The soil moisture fluctuation can be observed only in the surficial region between elevations of 641 ft to 634.37 ft and there is not any development of positive pore water pressure. Even after 10 days of rainfall event, significant improvement in soil strength parameters due to rehabilitation of clayey soil using 8% lime and minor changes in soil pore water pressure diagram leads to increase in the calculated minimum FOS (3.147).

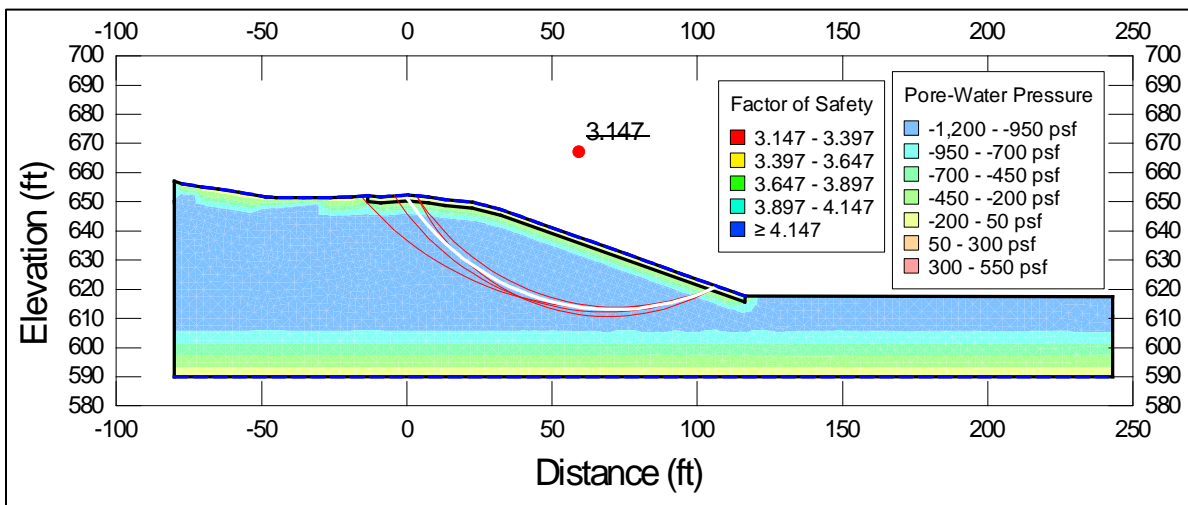
Table 5 presents the FOS values of the slope for the three analysis cases and different rainfall conditions. It can be concluded that the detrimental effects of wet-dry cycles on clayey soil can cause surficial slope instability problems under higher intensity and prolonged duration of rainfalls. However, rehabilitation of the clayey soil with lime improves soil strength parameters and results in sufficient FOS values of the slope for all the analysis.

**Table 5. Calculated FOS values after different rainfall amount for Texas site slope.**

<b>Case #</b>	<b>6.21 inches</b>	<b>8.22 inches</b>	<b>10.10 inches</b>
Case 1	2.839	2.838	2.838
Case 2	1.864	1.304	0.861
Case 3	3.185	3.167	3.147



(a)



(b)

Figure 19. (a) The pore water pressure distribution at the middle of the slope after 10 days of rainfall event (Case 3) and (b) calculated minimum slope FOS for lime treated slope.

## 6. CONCLUSIONS

The literature review and results of the research substantiate that the shear strength of Texas and Louisiana soils starts at peak strength and undergo significant strength loss when exposed to wet-dry weathering cycles over time to attain the Fully Softened Strength (FSS). Moreover, the saturated hydraulic conductivity increases by 2 to 4 orders of magnitude (i.e.,  $10^2$  to  $10^4$  times) due to the wetting and drying cycles. The reduction in soil strength from peak to FSS and an increase in hydraulic conductivity values provide valuable insight into the development of failure conditions in the embankment with time. For example, the results suggest that a newly compacted specimen of clayey soil has sufficient cohesion value (13.2 kPa) whereas, in fully softened condition, clayey soil significantly lost its cohesion (reduced to 1.28 kPa). The friction angle value did not vary from peak to fully softened state, which corresponds to work conducted by Stark and Eid (42). The results also show that the soils collected from Texas site experienced significant amounts of shrinkage, a typical property of expansive soils. A higher volumetric shrinkage causes more moisture infiltration during the wetting period after the drought, and it indicates a higher chance of getting drastically affected by shrinking and swelling phenomenon. This may subsequently contribute to the loss of cohesion, an increase in hydraulic conductivity values and eventually lead to failure of surficial slopes of the highway embankment. The numerical simulations show that the factor safety is still high for rainfall totals less than 6 inches. However, as the rainfall increases to over 10 inches, the factor of safety approaches unity (1.0), which indicates imminent failure. The long-term experiments are in their final stage of preparation and will be conducted over a long time period to fundamentally understand when compacted soil properties change with time.

## REFERENCES

1. Puppala, A. J., K. Punthutaecha, S. K. Vanapalli, and H. Inyang. Volume Change Behaviors of Expansive Soils Stabilized with Recycled Ashes and Fibers. *Journal of Materials in Civil Engineering*, Vol. 18, No. 2, 2006, pp. 295–306. [https://doi.org/10.1061/\(ASCE\)0899-1561\(2006\)18:2\(295\)](https://doi.org/10.1061/(ASCE)0899-1561(2006)18:2(295)).
2. Chakraborty, S., and S. Nair. Impact of Different Hydrated Cementitious Phases on Moisture-Induced Damage in Lime-Stabilised Subgrade Soils. *Road Materials and Pavement Design*, Vol. 19, No. 6, 2018, pp. 1389–1405. <https://doi.org/10.1080/14680629.2017.1314222>.
3. Chakraborty, S., and S. Nair. Impact of Curing Time on Moisture-Induced Damage in Lime-Treated Soils. *International Journal of Pavement Engineering*, 2018, pp. 1–13. <https://doi.org/10.1080/10298436.2018.1453068>.
4. Das, J. T., A. J. Puppala, T. V. Bheemasetti, L. A. Walshire, and M. K. Corcoran. Sustainability and Resilience Analyses in Slope Stabilisation. *Proceedings of the Institution of Civil Engineers - Engineering Sustainability*, Vol. 171, No. 1, 2018, pp. 25–36. <https://doi.org/10.1680/jensu.16.00054>.
5. He, S., X. Yu, A. Banerjee, and A. J. Puppala. Expansive Soil Treatment with Liquid Ionic Soil Stabilizer. *Transportation Research Record: Journal of the Transportation Research Board*, 2018, p. 036119811879299. <https://doi.org/10.1177/0361198118792996>.
6. Caballero, S., R. Acharya, A. Banerjee, T. V. Bheemasetti, A. J. Puppala, and U. Patil. Sustainable Slope Stabilization Using Biopolymer-Reinforced Soil. 2016.
7. Puppala, A. J., S. S. C. Congress, and A. Banerjee. Research Advancements in Expansive Soil Characterization, Stabilization and Geoinfrastructure Monitoring, pp. 15–29.
8. George, A. M., S. Chakraborty, J. T. Das, A. Pedarla, and A. J. Puppala. Understanding Shallow Slope Failures on Expansive Soil Embankments in North Texas Using Unsaturated Soil Property Framework. 2018.
9. Samuel, R., O. Huang, A. Banerjee, A. Puppala, J. Das, and M. Radovic. Biopolymers. 2019.
10. Das, J. T. *Evaluation of the Rate of Secondary Swelling in Expansive Clays Using Centrifuge Technology*. 2014.
11. Das, J. T., A. Banerjee, S. Chakraborty, and A. J. Puppala. A Framework for Assessment of Sustainability and Resilience in Subgrade Stabilization for a High-Volume Road. 2018.
12. Peron, H., L. Laloui, L.-B. Hu, and T. Hueckel. Formation of Drying Crack Patterns in Soils: A Deterministic Approach. *Acta Geotechnica*, Vol. 8, No. 2, 2013, pp. 215–221. <https://doi.org/10.1007/s11440-012-0184-5>.
13. Kayyal, M. K., and S. G. Wright. Investigation of Long-Term Strength Properties of Paris and Beaumont Clays in Earth Embankments. 1991.
14. Albrecht, B. A., and C. H. Benson. Effect of Desiccation on Compacted Natural Clays. *Journal of Geotechnical and Geoenvironmental Engineering*, Vol. 127, No. 1, 2001, pp. 67–75. [https://doi.org/10.1061/\(ASCE\)1090-0241\(2001\)127:1\(67\)](https://doi.org/10.1061/(ASCE)1090-0241(2001)127:1(67)).

15. Boynton, S. S., and D. E. Daniel. Hydraulic Conductivity Tests on Compacted Clay. *Journal of Geotechnical Engineering*, Vol. 111, No. 4, 1985, pp. 465–478. [https://doi.org/10.1061/\(ASCE\)0733-9410\(1985\)111:4\(465\)](https://doi.org/10.1061/(ASCE)0733-9410(1985)111:4(465)).
16. Puppala, A. J., D. Basu, O. Cuisinier, and J. T. Das. General Report of TC 307--Sustainability in Geotechnical Engineering. 2017, pp. 3353–3360.
17. Jafari, N. H., A. Puppala, B. Boluk, J. A. Cadigan, S. Chakraborty, T. Bheemasetti, and J. E. Pleasant. Predicting the Performance of Highway Embankment Slopes. *MATEC Web of Conferences*, Vol. 271, 2019, p. 02007. <https://doi.org/10.1051/mateconf/201927102007>.
18. Banerjee, A. *Response of Unsaturated Soils Under Monotonic and Dynamic Loading over Moderate Suction States*. Doctoral Dissertation, The University of Texas at Arlington, Arlington, Texas, 2017.
19. Banerjee, A., A. J. Puppala, U. D. Patil, L. R. Hoyos, and P. Bhaskar. A Simplified Approach to Determine the Response of Unsaturated Soils Using Multistage Triaxial Test. 2018.
20. Gamez, J. A., and T. D. Stark. Fully Softened Shear Strength at Low Stresses for Levee and Embankment Design. *Journal of Geotechnical and Geoenvironmental Engineering*, Vol. 140, No. 9, 2014, p. 06014010. [https://doi.org/10.1061/\(ASCE\)GT.1943-5606.0001151](https://doi.org/10.1061/(ASCE)GT.1943-5606.0001151).
21. Saleh, A. A., and S. G. Wright. *Shear Strength Correlations and Remedial Measure Guidelines for Long-Term Stability of Slopes Constructed of Highly Plastic Clay Soils*. 1997.
22. Fleming, R. L., G. L. Sills, and E. S. Steward. Lime Stabilization of Levee Slopes. 1992.
23. Day, R. W., and G. W. Axten. Surficial Stability of Compacted Clay Slopes. *Journal of Geotechnical Engineering*, Vol. 115, No. 41. Day, R. W., and G. W. Axten. Surficial Stability of Compacted Clay Slopes. *Journal of Geotechnical Engineering*, Vol. 115, No. 4, 1989, pp. 577–580. [https://doi.org/10.1061/\(ASCE\)0733-9410\(1989\)115:4\(577\)](https://doi.org/10.1061/(ASCE)0733-9410(1989)115:4(577))., 1989, pp. 577–580. [https://doi.org/10.1061/\(ASCE\)0733-9410\(1989\)115:4\(577\)](https://doi.org/10.1061/(ASCE)0733-9410(1989)115:4(577)).
24. Nelson, J. D., and D. J. Miller. *Expansive Soils : Problems and Practice in Foundation and Pavement Engineering*. J. Wiley, 1992.
25. Mitchell, J. K., K. Soga, and others. *Fundamentals of Soil Behavior*. John Wiley & Sons New York, 2005.
26. Day, R. W. Surficial Stability of Compacted Clay: Case Study. *Journal of Geotechnical Engineering*, Vol. 120, No. 11, 1994, pp. 1980–1990. [https://doi.org/10.1061/\(ASCE\)0733-9410\(1994\)120:11\(1980\)](https://doi.org/10.1061/(ASCE)0733-9410(1994)120:11(1980)).
27. Day, R. W. Surficial Slope Failure: A Case Study. *Journal of Performance of Constructed Facilities*, Vol. 7, No. 4, 1993, pp. 264–269. [https://doi.org/10.1061/\(ASCE\)0887-3828\(1993\)7:4\(264\)](https://doi.org/10.1061/(ASCE)0887-3828(1993)7:4(264)).
28. Day, R. W. Design and Repair for Surficial Slope Failures. *Practice Periodical on Structural Design and Construction*, Vol. 1, No. 3, 1996, pp. 83–87. [https://doi.org/10.1061/\(ASCE\)1084-0680\(1996\)1:3\(83\)](https://doi.org/10.1061/(ASCE)1084-0680(1996)1:3(83)).
29. Puppala, A. J., V. S. Dronamraju, L. Perrin, and K. L. McCleskey. Assessment of Field

- Stabilization Methods to Prevent Recurring Surficial Failures. *Proceedings of the 17th International Conference on Soil Mechanics and Geotechnical Engineering: The Academia and Practice of Geotechnical Engineering*, Vol. 2, No. 2005, 2009, pp. 1487–1490. <https://doi.org/10.3233/978-1-60750-031-5-1487>.
30. Wu, J. Y., K. Huang, and M. Sungkar. Remediation of Slope Failure by Compacted Soil-Cement Fill. *Journal of Performance of Constructed Facilities*, Vol. 31, No. 4, 2017, p. 04017022. [https://doi.org/10.1061/\(ASCE\)CF.1943-5509.0000998](https://doi.org/10.1061/(ASCE)CF.1943-5509.0000998).
  31. Puppala, A. J., B. C. S. Chittoori, N. Talluri, M. Le, T. Bheemasetti, and J. Thomey. Stabilizer Selection for Arresting Surficial Slope Failures: A Sustainability Perspective. 2013.
  32. McCleskey, K. L. J. *Experimental Investigations to Select Stabilization Methods to Mitigate Embankment Desiccation Cracks in Order to Reduce Slope Failures*. The University of Texas at Arlington, 2005.
  33. Chakraborty, S., J. T. Das, A. J. Puppala, and A. Banerjee. Natural Frequency of Earthen Dams at Different Induced Strain Levels. *Engineering Geology*, Vol. 248, 2019, pp. 330–345. <https://doi.org/10.1016/j.enggeo.2018.12.008>.
  34. Chakraborty, S., A. Banerjee, J. T. Das, L. Mosadegh, and A. J. Puppala. Impact of Variation of Small Strain Shear Modulus on Seismic Slope Stability Analysis of a Levee: A Sensitivity Analysis. 2018.
  35. Chakraborty, S., T. V. Bheemasetti, A. J. Puppala, and L. Verreault. Use of Constant Energy Source in SASW Test and Its Influence on Seismic Response Analysis. *Geotechnical Testing Journal*, Vol. 41, No. 6, 2019, p. 20170220. <https://doi.org/10.1520/GTJ20170220>.
  36. Chakraborty, S., T. V. Bheemasetti, and A. J. Puppala. Effect of Constant Energy Source on Coherence Function in Spectral Analysis of Surface Waves (SASW) Testing, pp. 59–65.
  37. USSD. *Strength of Materials for Embankment Dams, United States Society on Dams*. 2007.
  38. USACE. *Slope Stability Engineer Manual EM 1110-2-1902*. 2003.
  39. Skempton, A. W. First-Time Slides in Overconsolidated Clays. *Geotechnique*, Vol. 20, No. 3, 1970, pp. 320–324.
  40. Dronamraju, V. S. *Studies on Field Stabilization Methods to Prevent Surficial Slope Failures of Earthfill Dams*. The University of Texas at Arlington, 2008.
  41. Stark, T. D., and M. Hussain. Empirical Correlations: Drained Shear Strength for Slope Stability Analyses. *Journal of Geotechnical and Geoenvironmental Engineering*, Vol. 139, No. 6, 2013, pp. 853–862. [https://doi.org/10.1061/\(ASCE\)GT.1943-5606.0000824](https://doi.org/10.1061/(ASCE)GT.1943-5606.0000824).
  42. Stark, T. D., and H. T. Eid. Slope Stability Analyses in Stiff Fissured Clays. *Journal of Geotechnical and Geoenvironmental Engineering*, Vol. 123, No. 4, 1997, pp. 335–343. [https://doi.org/10.1061/\(ASCE\)1090-0241\(1997\)123:4\(335\)](https://doi.org/10.1061/(ASCE)1090-0241(1997)123:4(335)).
  43. Benson, C. H. Effect of Desiccation on Compacted Natural Clays. Vol. 0241, No. March, 2001. [https://doi.org/10.1061/\(ASCE\)1090-0241\(2001\)127](https://doi.org/10.1061/(ASCE)1090-0241(2001)127).
  44. Smethurst, J. A., K. M. Briggs, W. Powrie, A. Ridley, and D. J. E. Butcher. Mechanical and Hydrological Impacts of Tree Removal on a Clay Fill Railway Embankment. *Géotechnique*,

- Vol. 65, No. 11, 2015, pp. 869–882. <https://doi.org/10.1680/jgeot.14.P.010>.
45. Powrie, W., and J. Smethurst. Climate and Vegetation Impacts on Infrastructure Cuttings and Embankments. In *Proceedings of the 8th International Congress on Environmental Geotechnics Volume 1*, Springer Singapore, pp. 128–144.
  46. Benson, C. H., A. Sawangsuriya, B. Trzebiatowski, and W. H. Albright. Postconstruction Changes in the Hydraulic Properties of Water Balance Cover Soils. *Journal of Geotechnical and Geoenvironmental Engineering*, Vol. 133, No. 4, 2007, pp. 349–359. [https://doi.org/10.1061/\(ASCE\)1090-0241\(2007\)133:4\(349\)](https://doi.org/10.1061/(ASCE)1090-0241(2007)133:4(349)).
  47. Ishimwe, E., J. Blanchard, and R. A. Coffman. Field-Obtained Soil Water Characteristic Curves and Hydraulic Conductivity Functions. *Journal of Irrigation and Drainage Engineering*, Vol. 144, No. 1, 2018, p. 4017056. [https://doi.org/Artn0401705610.1061/\(Asce\)Ir.1943-4774.0001272](https://doi.org/Artn0401705610.1061/(Asce)Ir.1943-4774.0001272).
  48. Skempton, A. W. Slope Stability of Cuttings in Brown London Clay. In *Selected Papers On Soil Mechanics*, Thomas Telford Publishing, pp. 241–250.
  49. Wright, S. G., J. G. Zornberg, and J. E. Aguetant. *The Fully Softened Shear Strength of High Plasticity Clays. Project No. 0-5202-3, Center for Transportation Research, The University of Texas at Austin, (August 2007): 132 Pgs. 2007.*
  50. Bhaskar, P., B. Boluk, A. Banerjee, A. Shafikhani, and A. Puppala. Unsaturated Soils. 2019.
  51. van Genuchten, M. T. A Closed-Form Equation for Predicting the Hydraulic Conductivity of Unsaturated Soils<sup>1</sup>. *Soil Science Society of America Journal*, Vol. 44, No. 5, 1980, p. 892. <https://doi.org/10.2136/sssaj1980.03615995004400050002x>.
  52. David Suits, L., T. Sheahan, A. Puppala, B. Katha, and L. Hoyos. Volumetric Shrinkage Strain Measurements in Expansive Soils Using Digital Imaging Technology. *Geotechnical Testing Journal*, Vol. 27, No. 6, 2004, p. 12069. <https://doi.org/10.1520/GTJ12069>.
  53. Lee, L. M., N. Gofar, and H. Rahardjo. A Simple Model for Preliminary Evaluation of Rainfall-Induced Slope Instability. *Engineering Geology*, Vol. 108, No. 3–4, 2009, pp. 272–285. <https://doi.org/10.1016/j.enggeo.2009.06.011>.
  54. Perica, S., S. Pavlovic, M. S. Laurent, C. Trypaluk, D. Unruh, D. Martin, and O. Wilhite. NOAA Atlas 14: Precipitation Frequency Atlas of the United States Volume 10: Northeastern States.
  55. Zhang, F., and D. G. Fredlund. Examination of the Estimation of Relative Permeability for Unsaturated Soils. Vol. 2087, No. May, 2015, pp. 2077–2087.
  56. Hughes, P. N., S. Glendinning, J. Mendes, G. Parkin, D. G. Toll, D. Gallipoli, and P. E. Miller. Full-Scale Testing to Assess Climate Effects on Embankments. *Proceedings of the Institution of Civil Engineers - Engineering Sustainability*, Vol. 162, No. 2, 2009, pp. 67–79. <https://doi.org/10.1680/ensu.2009.162.2.67>.